applied sciences

MDPI

Review

Review of Visualization Technique and Its Application of Road Aggregates Based on Morphological Features

Lei Wang [1,2], Yongsheng Yao [1,2], Jue Li [1,3,*], Yiyang Tao [4] and Kefei Liu [5]

1 College of Traffic & Transportation, Chongqing Jiaotong University, Chongqing 400074, China
2 National & Local Joint Engineering Research Center of Transportation and Civil Engineering Materials, Chongqing Jiaotong University, Chongqing 400074, China
3 Key Laboratory of Special Environment Road Engineering of Hunan Province, Changsha University of Science & Technology, Changsha 410114, China
4 Zhongyuan Institute of Science and Technology, Zhengzhou 451450, China
5 School of Civil Engineering, Central South University of Forestry and Technology, Changsha 410004, China
* Correspondence: lijue1207@cqjtu.edu.cn

Abstract: The sustainable performance of asphalt pavement depends on the quality and mix design of road aggregates. Identifying aggregate morphology and size is a prerequisite step for material design and numerical modeling of asphalt mixtures. The paper aims to review the morphometric measurement, characteristic parameters and visualization technique of road aggregates. Types, calculation methods and advantages of aggregate morphological characteristics are highlighted. The applications of aggregate morphological features on the volumetric design, compaction processes, mechanical properties and size effect of asphalt mixtures are summarized. Although digital image processing technology has been studied for years, aggregates in the complex accumulation are still difficult to measure accurately. In the current research, the morphological parameters of aggregates remain diverse without a standard protocol. Compared to theoretical models, numerical models have more difficulties establishing irregular morphology features in the simulated specimens but provide a volume parameter closer to the real value. The future investigation of road performance under dynamic loading should account for the microscopic evolution of shape, orientation and distribution of aggregates over time.

Keywords: road aggregate; morphological feature; visualization technique; numerical method; mechanical property

Citation: Wang, L.; Yao, Y.; Li, J.; Tao, Y.; Liu, K. Review of Visualization Technique and Its Application of Road Aggregates Based on Morphological Features. *Appl. Sci.* **2022**, *12*, 10571. https://doi.org/10.3390/app122010571

Academic Editor: Giuseppe Lacidogna

Received: 25 September 2022
Accepted: 18 October 2022
Published: 19 October 2022

1. Introduction

Asphalt mixtures are used in over 90% of highway construction in China. Currently, asphalt pavement generally has a short service life, and there is a gap in the design life. Aggregates account for more than 90% of the total mass of asphalt mixtures. Mineral aggregate, a vitally important road material, forms a good load-bearing capacity after gradation combination and sufficient compaction and can be used directly in the paving of the subgrade or subbase of road structures [1]. At the same time, multiphase composites are structurally characterized by a coarse aggregate skeleton and fine aggregate filling through binders such as asphalt and cement [2]. These materials have long dominated the pavement structure. Using aggregate properties to improve their mixes' mechanical properties and service life has been an important area of research in road engineering.

Most of the existing mix design methods use macroscopic bulk indicators (bulk density, void ratio, effective asphalt content, etc.) and optimize the gradation composition by mechanical empirical methods [3]. However, the reliability and accuracy of their test results lack scientific and effective verification and evaluation methods. A mixture design method based on fine mechanics has been developed recently to break through the traditional empirical and continuum mechanics design concept [4]. The interaction mechanism of

aggregates, mortar and other components from the micro-factors of materials was explored by mechanical means to reveal the inner law of the mechanical properties change of the mixture for a more excellent mixture structure design [5]. Currently, researchers in various countries have carried out macroscopic and fine-scale studies in mechanical property tests and pavement structural response of pavement materials such as asphalt mixes [6,7] and cement concrete [8] and have successfully applied various mechanical analysis tools such as the analytical method [9], finite element method [10,11], and discrete element method [12]—all of which can further demonstrate the feasibility of the mix design of materials.

As early as the 1990s, researchers of the SHRP program in the United States realized that micro-factors of materials had a huge influence on the mechanical properties of the mixes and qualified the geometric characteristics of the aggregates (pinch content, angularity, fracture surface, etc.) [13]. In recent years, pavement workers have mostly analyzed aggregate shapes through two-dimensional digital images, yet their properties' complexity and variability are not limited to flat surfaces. The anisotropy of physical mechanics should also consider the variability of three-dimensional morphology [14]. With the introduction of X-ray computed tomography (X-ray CT) scanning technology, the computer performance and digital modeling of pavement engineering tend to mature, providing an effective way to accurately describe aggregates' properties and structural characteristics and their mixes. Therefore, this paper discusses the current research progress and main ftechnical challenges in aggregate visualization by integrating existing research and related results.

This paper reviews the techniques and numerical simulations for visualizing the morphological characteristics of road aggregates, especially asphalt mixtures. The development status of digital image acquisition equipment is summarized and introduced, including dynamic digital imaging techniques, static digital imaging techniques, and the influence of morphological characteristics of road aggregate on its fine structure and properties. The progress of visualizing the morphological characteristics of road aggregate is discussed. In addition, the evaluation methods and evaluation indexes from the shape, angularity and texture of aggregates are summarized and generalized systematically. In terms of numerical model reconstruction of aggregates, the modeling procedures of real aggregate models and random generation models are introduced, respectively. The numerical simulation methods, including discrete and finite element methods, in predicting mechanical properties, are reviewed. Moreover, the void fraction of the aggregate, the gradation design and the method of compaction of the specimens are taken into account, which is also affected by aggregate morphological characteristics. The application of the aggregate's shape in terms of its mechanical properties and size effect is outlined. The flow chart of this review is shown in Figure 1.

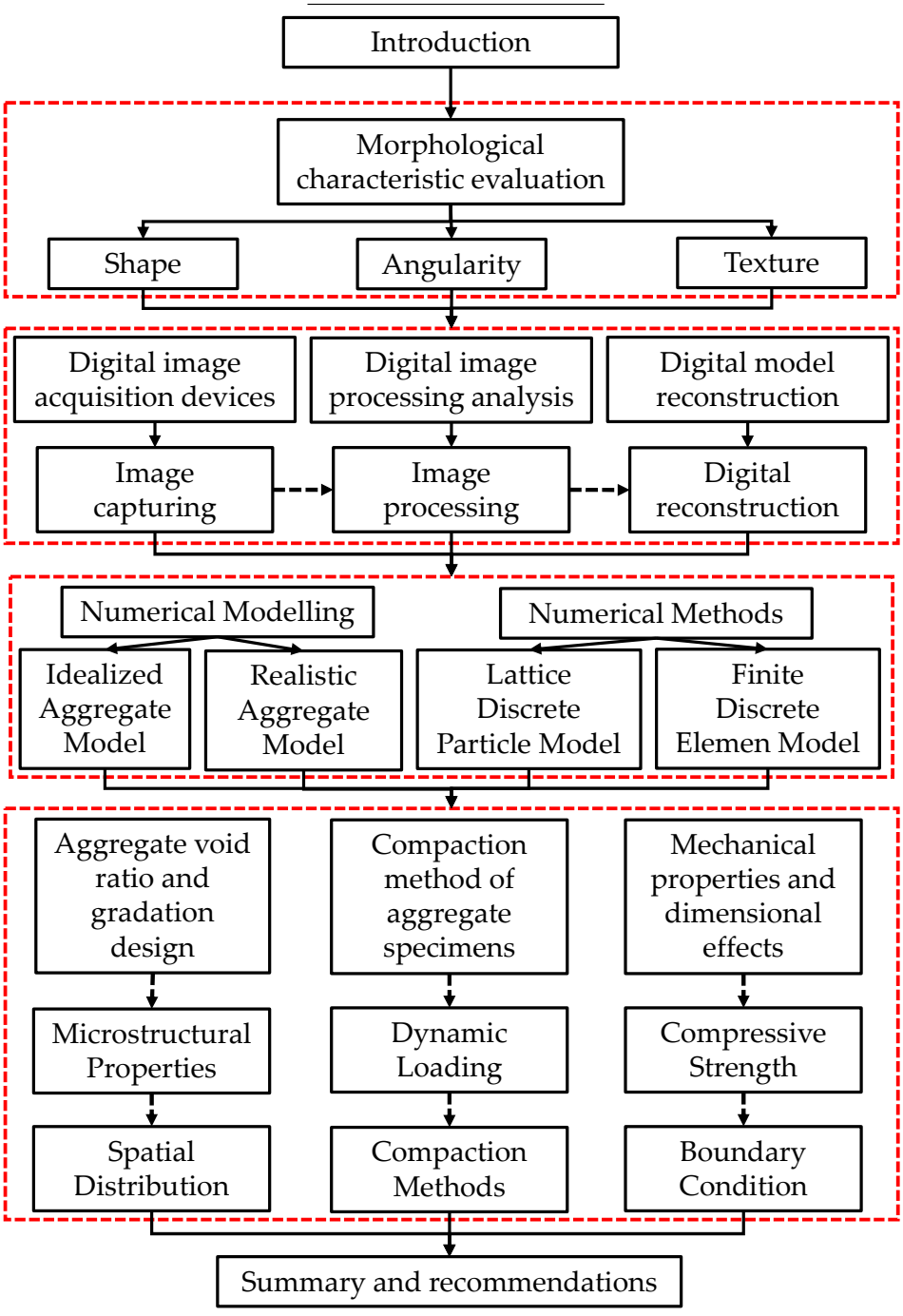

Figure 1. Flowchart of this review.

2. Morphological Characteristic Evaluation

The engineering properties of building materials (e.g., asphalt mixes and cement concrete) are influenced by the morphological characteristics (shape, angle, and texture) of the aggregates [15]. Therefore, suitable evaluation methods and indicators can better quantify the morphological characteristics of aggregates. Specifically, the shape profile and angularity of coarse aggregates belong to the macroscopic category, while the surface texture belongs to the microscopic category [16]. The relationship among shape, angularity and surface texture is shown in Figure 2.

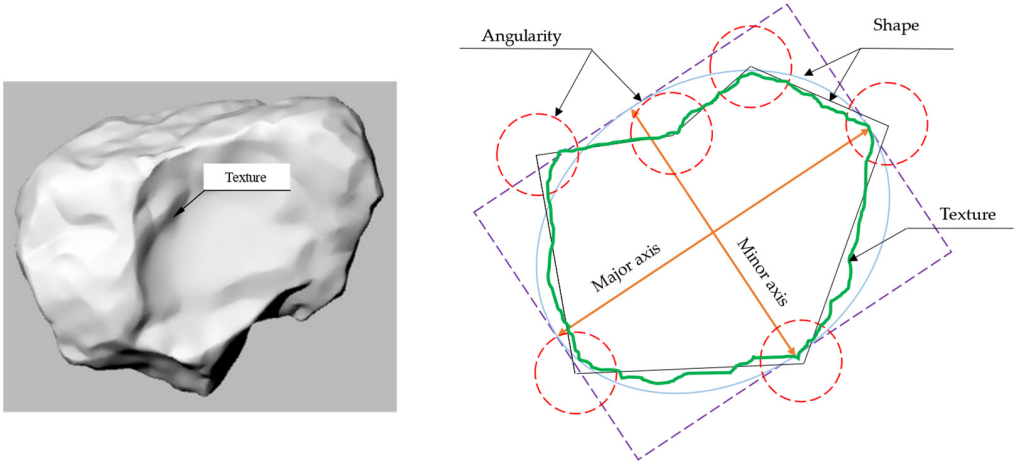

Figure 2. Relationship among shape, angularity and surface texture.

2.1. Shape

The shape of the aggregate can be divided into two dimensions and three dimensions, and the analysis of the aggregate shape can be divided into sphericity and shape factor, roundness, formation index, Fourier series, flat length ratio, aspect ratio, width ratio, symmetry, and three-dimensional shape factor [17]. As for the contour characteristics of particles, the concept of two-dimensional planes is mainly involved. With the development of digital image technology, the quantitative indexes of contour shape have progressed from shallow to deep, from the simple fine length to the development of relatively fine angular roundness. The fine length, also known as the axis ratio, is generally defined as the ratio of the long axis to the short axis of the equivalent ellipse of the planar projection of the aggregate.

The indicators characterizing the shape of the aggregates can be distinguished into 2D and 3D. Among them, most of the 2D metrics use length and area for shape characterization, such as form index (2D), roundness, the ratio of breadth to width, etc. It is easy to lose a lot of shape detail information. The aggregates' shape, angularity and texture are effectively separated by the Fourier series method. Three-dimensional indexes include shape factor (SF), flat and elongated ratio (FER), and sphericity (ψ). These indexes can characterize the aggregate morphology more accurately. The shape index of aggregate with calculation equations and main characteristics is shown in Table 1.

Table 1. Shape index of aggregate with calculation equations and main characteristics.

Shape Indexes	Equations *	Characteristics	Literatures
Form index (2D)	$\sum_{\theta=0}^{360-\Delta\theta} \frac{\lvert R_{\theta+\Delta\theta}-R_{\theta}\rvert}{R_{\theta}}$	Quantifying the 2D image of fine aggregates of relative form and using incremental changes in the particle radius. These parameters use the length and area method to characterize the shape of the aggregate; however, it loses a large amount of shape detail information	[18]
Aspect ratio (AR)	$\frac{D_{\max}}{D_{\min}}$		[19]
Rectangular degree (RD)	$\frac{A}{A_{MER}}$		[20]
Axial coefficient (AC)	$\frac{L_{\max}}{L_{\min}}$		[21]
Eccentricity (E)	$\frac{c}{a}$	Eccentricity could characterize the shape of the aggregate particles and reflect the elliptical oblate degree.	[19]

Table 1. *Cont.*

Shape Indexes	Equations *	Characteristics	Literatures
Roundness	$\frac{4\pi A}{L^2}$	Roundness was the inverse of the form factor. In early imaging techniques, it was used to calculate 2D features of particle shape.	[22]
Form index using Fourier series (FRFORM)	$R(\theta) = a_0 + \sum_{m=1}^{\infty} [a_m \cos(m\theta) + b_m \sin(m\theta)]$	Fourier series can be used to analyze the form, angularity, and texture of aggregate shape.	[23]
Form (shape) index(Fourier series)	$\frac{1}{2}\sum_{m=1}^{m=n_1}\left[\left(\frac{a_m}{a_0}\right)^2 + \left(\frac{b_m}{a_0}\right)^2\right]$		[23]
Ratio of Breadth to Width	$\frac{\min(x_c)}{\max(x_{Fe})}$	Breadth to width ratio can be used to describe the form of aggregate particles.	[24]
Symmetry	$\frac{1}{2}\left[1 + \min\left(\frac{r_1}{r_2}\right)\right]$	Symmetry is a term that some imaging systems use to describe aggregate form.	[24]
Shape Factor (SF)	$\frac{D_S}{\sqrt{D_L \times D_i}}$	Shape Factor was a typical index in a system that represented in terms of three dimensions (longest, intermediate, and shortest dimensions).	[25]
Flat and elongated ratio (FER)	$\frac{D_L}{D_S}$	FER represents the ratio between the longest dimension and the shortest dimension of a particle.	[26]
Sphericity (ψ)	$\sqrt[3]{\frac{D_S \times D_i}{{D_L}^2}}$	Sphericity is a 3D parameter, which can characterize the aggregate morphology more accurately.	[27]

* θ—directional angle; $\Delta\theta$—incremental difference in the angles; R_θ—radius of the particle at angle θ; $R_{\theta+\Delta\theta}$—radius of the particle at angle $\theta + \Delta\theta$. D_{max}—the maximum length of the minimum external rectangle of the aggregate profile; D_{min}—minimum size of the minimum external rectangle. A—Area of the aggregate profile; A_{MER}—area of minimum circumscribed rectangle. L_{max}—major axis length of equivalent ellipse; L_{min}—minor axis length of equivalent ellipse. c—focal length of ellipse with same second moment; a—major axis of the ellipse. L—Circumference of the aggregate profile. m—frequency; a_0—average radius; a_m, b_m—Fourier coefficients n_1—threshold frequencies separating shape and angularity. x_c—maximum chord; x_{Fe}—the Feret diameter. r_1, r_2—the distances of the center of gravity to the edge in a given direction. D_L—length, longest dimension; D_i—width, intermediate dimension, the maximum dimension in the plane perpendicular to the length; D_S—thickness, shortest dimension.

Mora et al. [28] proposed a method for measuring the sphericity, shape factor and convexity of concrete aggregates, which estimated the thickness and volume of the particles, measured the thickness-dependent shape parameters, and evaluated the weighted average of individual particle shape parameters in aggregate specimens. Al-Rousan et al. [29] evaluated the accuracy of the analytical methods used in currently available imaging systems. Komba et al. [30] reconstructed a three-dimensional model of aggregate particles after obtaining data from three-dimensional laser scans of various types of aggregates. This laser scanning technique can better quantify the morphological characteristics of aggregates by calculating the sphericity from surface area and volume, the sphericity from three orthogonal dimensions, and the flat-length ratio from the longest and shortest dimensions of the aggregate particles.

The brittleness index is an important shape parameter in aggregates widely used in infrastructure construction, such as roads, and Anochie-Boateng et al. [31] developed a new equation for the brittleness index and verified its reliability. Laser scanning technology provided more accurate evaluation results and improved the selection of construction aggregates compared to traditional evaluation methods. Pan [32] and Tutumluer [33] evaluated the surface characteristics of crushed and uncrushed aggregates in asphalt mixtures using the 3D laser scanning technique, which had a good correlation with the experimental results. Ge et al. [34] proposed the flatness elongation index, sphericity index and specific surface area to characterize various aspects of the morphological characteristics

of coarse aggregates and derived that small-size aggregates have a larger proportion of elongated particle number.

From the above research, it can be seen that the 3D scanning technique can well-characterize the aggregate's shape. However, previous studies using 3D scanning technology have mainly focused on the shape, volume, and surface properties of aggregates from one or different quarries, with less research on the morphological decay pattern of aggregates during application.

2.2. Angularity

Aggregate angularity essentially describes the degree of sharpness of the angles. Corner roundness was proposed by Wadell [35] and others to describe the sharpness of the combination of corners and edges of a particle and was generally considered to be related to the radius of curvature or geometric fractal of the particle profile at the sharp end, while for quantitative evaluation, most researches have used the method of fitting similar polygons to obtain the angularity parameter of an aggregate. Fractals were first created by Mandelbrot [36] and have been widely used in various disciplines through continuous development. Fractals are used as a theoretical tool to describe and evaluate some characteristics such as hierarchical continuity, irregularity or randomness [37], and asphalt mixtures exhibit statistical self-similarity in volume and properties, which is suitable for quantitative analysis with fractal theory.

Wang et al. [38] proposed a unified Fourier morphological analysis method to quantify the shape characteristics of aggregates. Zhang et al. [39] proposed an index to characterize the combined effect of rib angle and surface texture of coarse aggregates, i.e., AT, and investigated the statistical distribution pattern of the AT index for different grain sizes of basalt aggregates and their composite aggregates. Rajan et al. [40] studied the comparison of rib angles of different grain sizes of aggregates under different crusher production. The angularity index of aggregate with calculation equations and main characteristics is shown in Table 2.

Table 2. Angularity index of aggregate with calculation equations and main characteristics.

Angularity Indexes	Equations *	Characteristics	Literatures
Angularity	$\frac{1}{2}\sum_{m=n_1+1}^{m=n_2}\left[\left(\frac{a_m}{a_0}\right)^2+\left(\frac{b_m}{a_0}\right)^2\right]$	Fourier series analysis was applied to measure the angularity of aggregate in PIAS.	[38]
Angularity factor (AF)	$AF=\sum_{p=1}^{N_A}\sum_{q=1}^{N_A}\left[\left(\frac{a(p,q)}{a_0}\right)^2+\left(\frac{b(p,q)}{a_0}\right)^2\right]$	The fast Fourier transform method could be applied to calculate and analyze the angularity factor (AF) of aggregate in FTI.	[41]
Surface erosion-dilation method	$\frac{A_1-A_2}{A_1}\times 100\%$	As a popular image processing technique, erosion dilation was utilized to analyze the angularity of aggregate particles in the UIAIA.	[42]
Gradient angularity (GA)	$\frac{1}{\frac{n}{3}-1}\sum_{i=1}^{n-3}\lvert\theta_i-\theta_{i+3}\rvert$	Higher values of GA indicate more angular aggregate particles.	[43]
Angularity index (AI) (radius)	$\sum_{\theta=0}^{\theta=360-\Delta\theta}\frac{\lvert R_{p\theta}-R_{EE\theta}\rvert}{R_{EE\theta}}\theta$	As the defining equation of angularity.	[27]
3D angularity (3DA)	$\frac{1}{3}\frac{\sum_{i=1}^{n_t}\frac{P_{ti}\cdot A_{ti}}{P_{te}}}{\sum_{i=1}^{n_t}A_{ti}}+\frac{\sum_{i=1}^{n_r}\frac{P_{ri}\cdot A_{ri}}{P_{re}}}{\sum_{i=1}^{n_r}A_{ri}}+\frac{\sum_{i=1}^{n_f}\frac{P_{fi}\cdot A_{fi}}{P_{fe}}}{\sum_{i=1}^{n_f}A_{fi}}$	3D parameters for more accurate characterization of aggregate morphology.	[43]

Table 2. *Cont.*

Angularity Indexes	Equations *	Characteristics	Literatures
Angularity parameter	$\left(\frac{p_{convex}}{p_{ellipse}}\right)^2$	All of them optimize the profile of the particles of the aggregate but cannot retain the original morphological characteristics of the aggregate.	[44]
Convexity	$\sqrt{\frac{A_{particle}}{A_{convex}}}$		[45]
Average angularitycoefficient	$I = \frac{\sum_{i=1}^{n} P_i \times I_{ai}}{100}$		[46]

* n_1, n_2—threshold frequencies separating shape, angularity, and texture. N_A—threshold value; N—size of $z(x,y)$ matrix; a, b—the real and imaginary roots of FFT2 coefficients; a_0—the average value of $z(x,y)$. A_1—initial area (in pixel) of 2D projection of particle in the image; A_2—area (in pixel) of the particle after performing a sequence of 'n' cycles of erosion—dilation. θ—directional angle; i—the ith point on the boundary of aggregate; n—total number of the points on the boundary of aggregate. $R_{p\theta}$—radius of the particle at a directional angle θ; $R_{EE\theta}$—radius of an equivalent ellipse at the same θ. P_{ti}, P_{ri}, P_{fi}—the parameters of grain particles; P_{te}, P_{re}, P_{fe}—the equivalent ellipse perimeters of grain particles; A_{ti}, A_{ri}, A_{fi}—the areas of grain particles; n_t, n_r, n_f—the total number of CT images, i—the ith CT image. p_{convex}—perimeter of an equivalent ellipse; $p_{ellipse}$—perimeter of the bounding polygon. $A_{particle}$—area of the real projection of aggregate; A_{convex}—area of convex aggregate's projection. P_i—mass percentage composition of each grade of particle size; I_{ai}—angularity coefficient of each grade of particle size.

Liu et al. [47] reconstructed the microstructure model of the asphalt mixes used for uniaxial compression tests based on X-ray CT scans, keeping the original morphology of the aggregates. The 3D finite element model with different aggregate angles was established and simulated for uniaxial compression tests by artificially reducing the aggregate angles by keeping the original morphology unchanged. The effect of the aggregate angle on the mechanical response of the asphalt mixture was quantitatively analyzed. In order to obtain the probability distribution of shape features, *GA* values were proposed in the previous study to quantify the 2D morphology of agglomerate particles by AIMS tests. The *GA* values of the aggregates are shown in Figure 3.

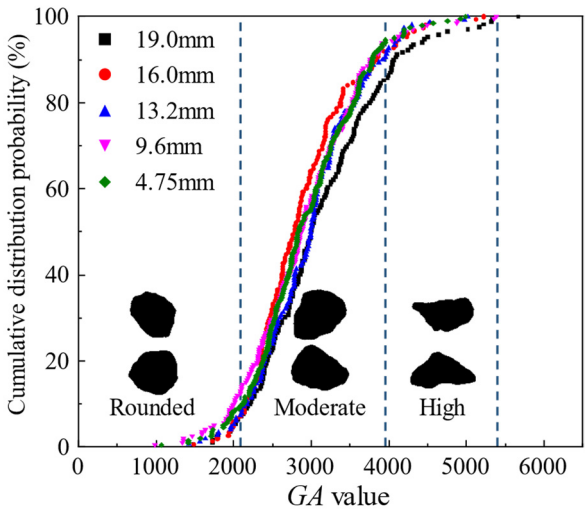

Figure 3. Distribution of *GA* values for aggregates.

Zhu et al. [48] collected the aggregate characteristics by a 3D blue-ray scanner, and evaluated the effect of coarse aggregate size and angles on the volumetric properties of asphalt mixtures. Huang et al. [49] prepared mixes with similar aggregate gradation using five different angular levels of coarse-grained aggregates and three different asphalt binders and evaluated the coarse aggregate angles (CAA) by compacted voids in coarse aggregates (VCA) and triaxial shear tests.

In summary, researchers have proposed various evaluation indicators to further improve the road performance of road aggregates from different angles by studying the angularity of aggregates. Currently, many shape indices have been proposed by mathematical methods. However, most of the studies of these indices are based on graphical

and statistical laws. Their correlation with the mechanical properties of aggregates lacks research. At the same time, the applicability of these indices for the prediction of the structural properties of the mixture still lacks a uniform classification standard.

2.3. Texture

The aggregate texture is mainly distinguished by the smoothness and roughness of aggregate particles. Miller et al. [50] proposed an analytical method to describe the surface texture of asphalt pavements using laser profiles to estimate friction characteristics. Al-Assi et al. [51] used Close-Range Photogrammetry (CRP) to measure the changes in micro texture on asphalt pavements. Khasawneh et al. [52] proposed an equation based on nonlinear regression to calculate the texture of asphalt pavements and the steady state's texture features. Du et al. [53] utilized a 2D wavelet method to describe the texture obtained by a 3D laser scanner on asphalt pavement. Hu et al. [54] conducted an analysis of the influence of texture on the skid resistance of asphalt pavements by using the collected pavement surface texture data. The texture index of aggregate with calculation equations and main characteristics is shown in Table 3.

Table 3. Texture index of aggregate with calculation equations and main characteristics.

Texture Indexes	Equations *	Characteristics	Literatures
Texture factor (TF)	$\sum_{p=1}^{N}\sum_{q=1}^{N}\left[\left(\frac{a(p,q)}{a_0}\right)^2+\left(\frac{b(p,q)}{a_0}\right)^2\right]-AF$	Fast measurement of aggregated morphological features based on 2D fast Fourier transform.	[55]
Texture index (TI)	$\frac{1}{3N}\sum_{i=1}^{3}\sum_{j=1}^{N}\left(D_{i,j}(x,y)\right)^2$	Quantization of textures using wavelet methods.	[55]
Erosion dilation area ratio (EDR)	$\frac{A_1-A_2}{A_1}\times 100\%$	Changes in area after erosion and dilatation cycles are directly related to aggregate texture.	[56]
Comprehensive erosion dilation area ratio (CEDR)	$\frac{\sum_{i}^{n}(a_i\times EDR_i)}{\sum_{i}^{n}a_i}$	Aggregate gradation is considered.	[57]
Surface texture	$\sum_{m=n_2+1}^{m=n_3}\sqrt{{a_m}^2+{b_m}^2}$	The shape, angularity and texture of the aggregates are considered separately.	[38]
Fourier series analysis method	$\frac{1}{2}\sum_{m=n_2+1}^{m=\infty}\left[\left(\frac{a_m}{a_0}\right)^2+\left(\frac{b_m}{a_o}\right)^2\right]$	Calculation of the surface fabric of aggregates used in PIAS.	[23]
Direct measurement of aggregate dimensions	$\left(\frac{P}{P_{convex}}\right)^2$	For evaluating textures, the texture parameters are related to the perimeter.	[44]
Three-dimensional Texture (MT_{3D}SHF)	$MT_{3D}=\sum_{n=26}^{n_{max}}\sum_{m=-1}^{n}\lvert a_{nm}\rvert$ $MT_{3DN}=\frac{MT_{3D}}{a_{00}}$	3D textures can be calculated.Can differentiate between aggregates with similar sizes.Used to compare aggregates of different sizes and volumes.	[58]

* N—the level of decomposition; i—a value of 1, 2, or 3 for the three detailed images of texture; j—the wavelet coefficient index. A_1—the 2D profile area of the aggregate; A_2—the 2D profile area of the aggregate after the erosion and expansion. a_i—the proportion of the ith grade aggregate in the gradation; EDR_i—erosion expansion area ratio of the ith grade of aggregate in the sample. P—the perimeter of a particle measured on a black and white image; P_{convex}—the perimeter of a bounding polygon. MT_{3D}—3D microtexture.

An asphalt mixture is a typical non-homogeneous composite material consisting of irregularly shaped and distributed aggregates, asphalt binder and voids [59,60]. The aggregate morphological characteristics significantly influence the properties of asphalt mixtures [61,62], which can be found in existing studies. Improving the performance of asphalt mixes based on morphological characteristics of aggregates accounting for 90% of the total mass of asphalt mixes is an important research direction. Traditional methods of testing aggregate morphological characteristics are time-consuming and rely heavily on subjective judgments, resulting in imprecise experimental results. In most of the tests,

it is difficult for the researchers to control the aggregate morphological characteristics variables [63]. Aragão et al. [64] mixed aggregates from different sources and tested them using AIMS to obtain aggregates with different angles and textures; nevertheless, it was impossible to distinguish which morphological characteristics were responsible for the effect. Wang et al. [65] employed a modified Los Angeles (LA) wear test to obtain aggregates with different angles, calculated the fractal dimension and changed the size and surface texture of the aggregates. Puzzo et al. [66] proposed a 3D model evaluation method for pavement texture based on digital image processing techniques, which used photographs to generate a Digital Surface Model (DSM) to calculate the digital Mean Texture Depth (MTD) and calculate and analyze other texture parameters for contour extraction.

Cui [55] evaluated the effect of aggregate morphology variation on the performance of asphalt pavements and investigated the asphalt coverage ratio and the mechanical properties of the mixture for different types of aggregates to quantify the aggregate morphological characteristics by AIMS. An accurate definition of the aggregate morphological characteristics is important for the initial design phase of pavements, extending the service life of roads and reducing the use of natural aggregates and the generation of solid waste.

Inadequate adhesion between asphalt and aggregate can cause severe distress in pavement structure and service life [67], and the conventional approach, which does not consider active adhesion mechanisms, is hardly convincing. Cui et al. [68] investigated and designed an active adhesion-based test method to compensate for the adhesion deficiency and used digital image processing techniques to quantify the adhesive properties. The results showed that digital image processing could measure the asphalt coating ratio accurately and effectively.

In summary, the texture is a micro-morphological characteristic of the aggregate. The greater the complexity of the surface texture, the greater the internal friction angle that can be generated when the aggregates are embedded and locked with each other after crushing. Aggregate texture has fewer means of characterization relative to shape and angularity. At present, there is no excellent way to judge the state of the textural distribution of asphalt pavement surface texture. Further development of evaluation metrics is needed to better predict pavement friction performance.

3. Digital Image Acquisition, Processing and Modelling Reconstruction

Asphalt mixtures contain anisotropic multiphase granular materials, including coarse aggregate, fine aggregate, asphalt, and voids [69]. The mechanical properties of asphalt mixture, a multiphase granular material, are related to its spatial structure, such as the distribution of coarse aggregate, the contact behavior between aggregate particles, the size and distribution of voids, etc. Coarse aggregate is one of the main components of the asphalt mixture, accounting for 50% to 80% of the total mass. In addition, its morphology, including shape, angularity and texture, significantly influences the performance of asphalt mixtures [16]. A great deal of research on the morphological features of coarse aggregates from various aspects has been conducted.

In recent years, the development of hardware and software for digital image processing and analysis has provided powerful tools for quantitative analysis as well as for studying the microstructure of aggregates [70]. Visualization is used as an important tool to study the internal structure of asphalt mixes [71]. This section will summarize digital image acquisition devices, digital image processing analysis and digital modelling reconstruction in turn. The strengths and weaknesses of these techniques are systematically summarized, as well as current problems with the subject and future work that must be addressed are highlighted.

3.1. Digital Image Acquisition Devices

Early digital imaging devices, usually relatively inexpensive microcomputers and digitizers collected the required data to analyze and measure the shape, surface area, and roughness of the aggregates and edited the data in combination with AutoCAD and Basic

programs to present them in the form of graphs, tables, and histograms [72]. This type of device can only measure the shape of the aggregate, and its accuracy is relatively low. It is clear that due to the limited technology and equipment available in the early days, it was impossible to characterize the angularity and texture of the aggregates. Among dynamic digital imaging methods, the VDG-40 particle classification video system from EMACO, Canada [73], can detect aggregates ranging in size from 1.18 mm to at least 37.5 mm, and capture 2D images of aggregates by calculating their length and width with a line-scan charge-coupled device (CCD) camera. However, the identification results can be heavily biased when the shape of the aggregate varies considerably. The computerized Particle Analyzer (CPA), which can be used in the laboratory and industrial production, applies dimensional and shape-based methods to analyze and process aggregate images [74]. The Micrometric Optisizer Particle Size Distribution Analyzer (PSDA) is used to analyze the aggregate shape by spherical and cubic methods [74]. PSDA is slow to image and captures only a fraction of the aggregates to analyze the particle size gradation. In the Video Image System (VIS), a sample holder is used to hold and move a large number of aggregates to a vibrating chute, and images of aggregates falling are captured by a CCD camera, which was further analyzed in the VIS system to generate a report. PSSDA is also able to provide information on the shape of the aggregates. The difference is that there are two systems for measuring the properties of coarse aggregates and fine aggregates, respectively. The Camsizer system captures digital images with two cameras, one taking images of coarse aggregates and the other one detecting fine particles. The Camsizer generally performs well in terms of analysis speed and accuracy, but its repeatability is relatively poor. The WipShape system, generally used for coarse aggregate analysis, has the ability to quickly analyze many aggregates. Size distribution curves and shape measurements are output by size category. Angles can be output through the minimum average curve radius method. Camsizer and WipShape acquired images of aggregates using two CCD cameras. However, these two techniques differ from each other in terms of instrumentation setup. 2D data is generated by Camsizer to determine the shape, whereas WipShape can capture images from two orthogonal views through two cameras separately, thus generating 3D shape information. The different methods presented above all use line scan CCD cameras to measure aggregates under backlight, while the difference between them lies in the physical configuration and software packages.

The imaging techniques for analyzing morphological features are described in Table 4, including early digital, dynamic, and static imaging techniques. The range of aggregate sizes applicable to each technology is presented. The morphological calculation methods corresponding to these techniques are also collected. Obviously, with the development of image technology, aggregates have been extensively studied. The camera setup in different techniques also varies greatly. Therefore, the advantages and disadvantages of these imaging techniques are summarized in Table 5.

Table 4. Characteristics of different imaging techniques.

Imaging Techniques		Aggregate Size Range	Morphological Calculation Methods			Literatures
			Shape	Angularity	Texture	
Early digital imaging devices		No.8-1-inch	Shape	-	-	[72]
Dynamic imaging techniques	VDG-40	No.16 to 1.5 inch	Length and width	-	-	[74]
	CPA	No.140 to 1.5 inch	Gradation and aspect ratio	-	-	[75]
	PSDA	No.200 to 1.5 inch	Shape, and gradation	-	-	[76]

Table 4. *Cont.*

Imaging Techniques		Aggregate Size Range	Morphological Calculation Methods			Literatures
			Shape	Angularity	Texture	
Dynamic imaging techniques	VIS	No.16 to 1.5 inch	Shape	-	-	[76]
	PSSDA	No.200 to 1.5 inch	Grading	-	-	[76]
	Camsizer	No.50 to 0.5 inch	Sphericity and aspect ratio	-	-	[45]
	WipShape	No.4 to 1.0 inch	Grading and aspect ratio	Minimum average curve radius method	-	[77]
	UIAIA	No.4 to 1.5 inch	Sphericity and aspect ratio	Change of outline slope	Erosion and dilation technique	[78]
Static imaging techniques	LAAS	No.10 to 4.0 inch	Aspect ratio	Wavelet method		[26]
	AIMS II	No.200 to 1.0 inch	Sphericity and aspect ratio	Gradient method	Wavelet method	[79]
	FTI system	No.50 to 0.75 inch	Sphericity and aspect ratio	Two-dimensional Fourier transform method		[80]
	PIAS	No.200 to 1.0 inch	Fast Fourier transform method			[23]
	OSAAS	No.16 to 5.0 inch	Sphericity, aspect ratio, and Spherical Harmonic Series	Wavelet method and Spherical Harmonic Series (SHS)		[81]
	X-ray CT	No.200 to 5.0 inch	Spherical Harmonic Series			[81]

Table 5. Advantages and Disadvantages of Imaging Techniques.

Imaging Techniques		Camera Setup	Advantages	Disadvantages
Early Imaging method		Digitizer with microcomputer	Measures shape.	No angularity or texture addressed.
Dynamic imaging techniques	VDG-40	One line-scan CCD camera	Measures shape of large aggregate quantity.	Assume idealized ellipsoid is a particle shape; cannot measure angularity and texture; use one camera magnification to take images of all aggregate sizes.
	CPA			
	PSDA			Separate vibratory feed systems and backlights required to scan fine and coarse samples.
	VIS			
	PSSDA		Measures shape of aggregates.	Two-dimensional shape information; no angularity or texture addressed.

Table 5. *Cont.*

Imaging Techniques		Camera Setup	Advantages	Disadvantages
Dynamic imaging techniques	Camsizer	Two digital cameras	Measures shape of large aggregate quantity. Use two cameras to capture images at different magnifications depending on the size of the collection.	Expensive. Assume the idealized ellipsoid as particle shape. No texture addressed.
	WipShape	Two orthogonal cameras	3D measurement of the shape of large aggregates.	No texture addressed. Use one camera magnification to take images of all aggregate sizes.
	UIAIA	Three orthogonal positioned cameras	3D measurement of the shape of large aggregates.	Use one camera magnification to take images of all aggregate sizes.
Static imaging techniques	LAAS	One CCD camera	Measure three dimensions of aggregates.	Use the same scan to analyze aggregates with different sizes.
	AIMS II	One camera with microscope	Capture images at different resolutions with a microscope depending on the size of the aggregates.	Expensive.
	FTI system	One CCD camera	Measuring three dimensions of aggregates with 3D image data.	Use the same scan to analyze aggregates with different sizes.
	PIAS	One digital camera	Measure shape, angularity, and texture. Acquire images using different scanning methods depending on the size of the aggregate.	The calculation is based on the 2D outline of aggregates.
	OSAAS	Two digital cameras	Measurement of 3D points on the aggregate surface.	Expensive. Use the same camera to analyze all sizes. Measure the shape of relatively small amounts of aggregates.
	X-ray CT	X-ray	Obtain the voxels of aggregate.	Expensive. Complicated operation.

At present, various technological means, such as high-definition digital cameras, electron microscopes, laser scanners and X-ray CT, are being applied in the field of particle morphological characterization, among which the relatively mature aggregate testing systems is the Aggregate Image Measurement System (AIMS) testing system created by the University of Illinois, USA [79]. Mahmoud et al. [82] developed AIMS and analyzed the stability of 3D dimensional measurements of coarse aggregates using X-ray CT scans for comparison. To verify the accuracy of the AIMS measurements, they used a wide selection of angular and textural indicators. Simultaneously, the true 3D dimensions of the aggregates were obtained using the X-ray scanning technique. The improved AIMS measurement method not only provides a fresh classification of aggregate particles in a sample but also automates the analysis process of aggregates, which is a positive point. Subsequent studies can incorporate statistical methods to further improve the technique. Rezaei et al. [83]

proposed another improved Aggregate Image Measurement System (AIMS II), which uses a closed dark box to eliminate the influence of ambient light and LED technology to overcome the disadvantage of difficult control of light intensity. The AIMS II automatically captures different resolutions of images according to the size of the aggregates through its digital camera with an autofocus microscope. The system is able to measure the 3D size of aggregates to determine parameters such as sphericity and aspect ratio and calculates the aggregates' angularity of various sizes by the gradient method and coarse aggregates texture by the wavelet method. The Fourier Transform interferometry system (FTI) uses a CCD camera to capture the aggregate images, which further generates the 3D coordinates of the aggregate top surface, whose shape is determined by the sphericity, flatness ratio and elongation. Wang et al. [84] compared the characteristics of different aggregate image measurement techniques and quantified the morphological features of different types of aggregates using AIMS II, a first-generation University of Illinois aggregate image analyzer (UIAIA), and a FTI system. The three aggregate imaging systems were evaluated. The results show that AIMS II provides a more direct and scientific measurement of the aggregate morphological features than traditional methods. AIMS has objectivity and reliability and can perform an accurate and comprehensive analysis of aggregate morphological characteristics and pavement texture characteristics. The X-ray CT 3D reconstruction system for aggregates has been designed and developed in the last 20 years [85]. CT technology obtains a series of perspective projection maps of the sample at different angles through the relative motion between the X-ray source, the sample and the detector, and a series of virtual slice maps of the sample interior by the 3D reconstruction algorithm, so as to complete the digital reconstruction of the 3D structure of the sample [86,87]. The core of CT technology is the theory related to image reconstruction from projection data, i.e., the inverse calculation of the line attenuation coefficient of X-rays corresponding to each point on the imaging plane from the projection data obtained from the scan. The CT device, AIMS system and laser scanner are shown in Figures 4 and 5, respectively.

The quantitative characterization of two-dimensional shape parameters of aggregates using digital image acquisition equipment and digital image processing techniques is one of the current hot spots in the study of morphological characteristics of aggregates [88].

In this subsection, we review the visualization techniques for road aggregates. Recent advances in digital image acquisition devices and techniques have been presented. Summarize how these image techniques adapt to the range of aggregate particle sizes and morphological characteristics of the aggregate as a whole. It is considered to be useful for the subsequent study of the effect of aggregate size on its properties. In addition, the advantages and disadvantages of the mentioned techniques are systematically and comprehensively discussed and summarized in favor of the development of aggregate morphology for road performance evaluation.

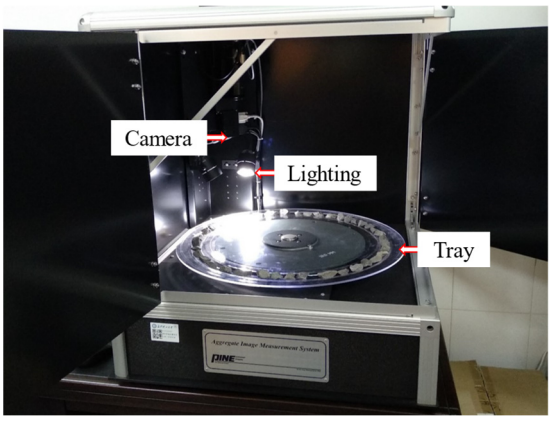

Figure 4. AIMS system.

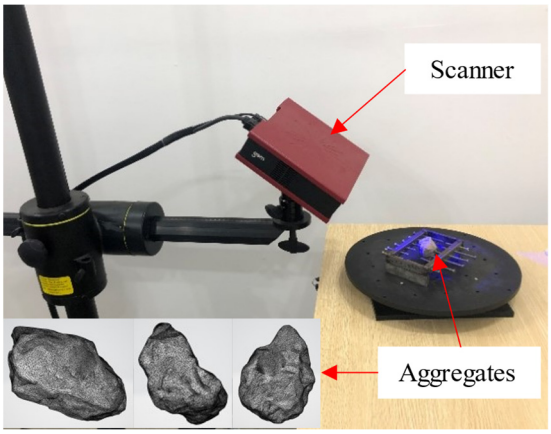

Figure 5. The laser scanner.

3.2. Digital Image Processing Analysis

Digital image processing (DIP) techniques extract important information from images by converting video images into digital form and applying various mathematical procedures. Various fields, such as biology, medicine, and materials science, have applied digital image technology. DIP techniques have enabled the microstructure of aggregates and their engineering properties to be analyzed with proficiency through image recognition and reproduction techniques [89]. DIP techniques involve four steps, namely digitization, enhancement, recovery, and segmentation [90].

The morphological properties of aggregates have been thoroughly analyzed and sufficiently explored to reveal the mechanisms between the complex structural features and the mechanical properties of aggregates. Eventually, the relation between material composition and mechanical properties was established from macroscopic and microscopic perspectives. The DIP method effectively assists in investigating the internal structural properties of aggregated particles. Figure 6 shows a schematic diagram of the process of 2D aggregate identification.

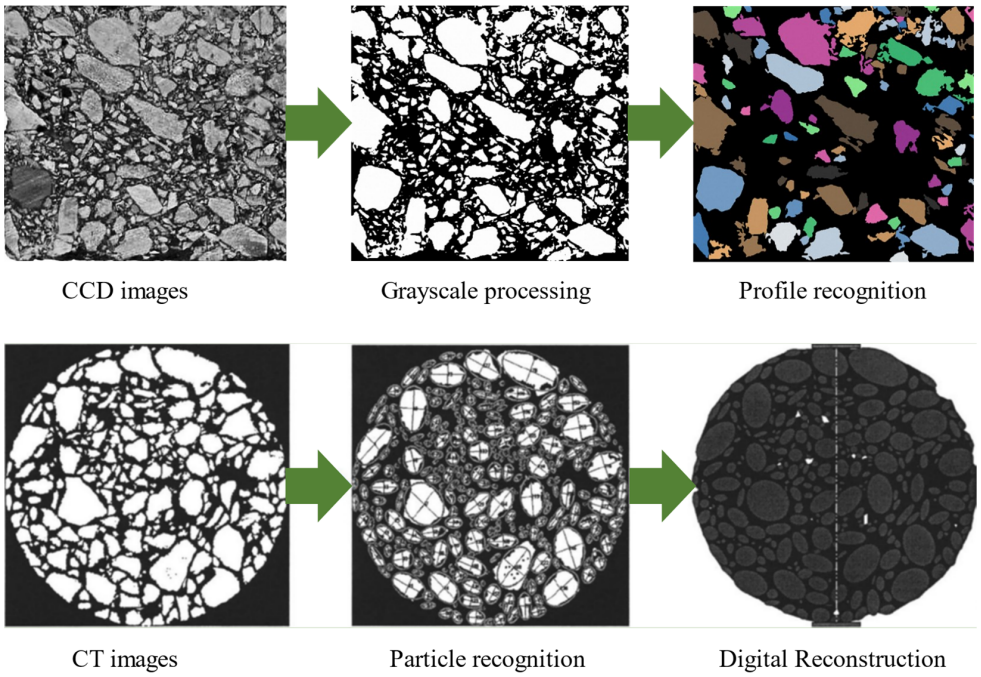

Figure 6. Schematic diagram of 2D aggregate particle identification.

Prudêncio et al. [91] proposed a simplified DIP based on the concept of volume factor to measure the particle shape index of fine aggregates. Scanning the aggregate image by distinguishing different resolution values, the volumetric coefficient of the aggregate was varied while the scan resolution was varied, and the value of the volumetric coefficient was stabilized at 300 dpi. Subsequently, a size correction factor "C" was proposed by comparing the manual measurement with the DIP technique. The results show that the actual largest size is equal to the multiplication of the DIP largest size and "C". The image processing technique further validates the accuracy of the test. However, there is an uncertainty in the correction factor for the volumetric coefficients presented in this study, which is limited by the particle shape.

Li et al. [92] used image technology to characterize shape indices such as elongation (ER), flatness ratio (FR), flatness and elongation coefficient (FEC), sphericity coefficient (SC), angle index (AI) and equivalent elliptical perimeter ratio (EEPR), and further investigated the effect of coarse aggregate morphological characteristics on the performance of heavy hot mix asphalt (HMA) pavements.

After vibratory compaction of the asphalt mixture, there is an uneven distribution of aggregates on the surface, which may lead to pavement segregation. The motion and rutting mechanism of coarse aggregates under load were analyzed in depth by Shi [70]. The movement characteristics of coarse aggregates in different asphalt mixtures and the correlation between the movement fine-scale parameters and the rutting depth were analyzed from the fine-scale perspective. The mechanical properties and service life of asphalt pavement, etc., are directly influenced by the degree of homogeneity of the asphalt mixture.

Cong et al. [93] proposed an image classification separation detection method for asphalt mixtures during construction, which used image processing methods to evaluate pavement segregation and effectively predict the degree of segregation during the paving process. The texture features in IPM are obtained by the DIP technique and combined with the Naïve Byers classification algorithm to classify the isolation state of images of compacted asphalt pavement (ICP). It provides a promising solution for the segregation evaluation of asphalt pavement construction and management. The overall accuracy of the proposed method is 87.50%, which is a significant improvement over manual detection.

Accurate characterization of the aggregate morphology is significant for the initial design phase of the pavement. Cui et al. [55] studied 9.5~13.2 grades of limestone and basalt by dividing different aggregate prism angles. In addition, the accurate aggregates' morphological characteristics can be quantified by AIMS. The angularity and sphericity of the aggregate are varied to allow for changes in the Marshall stability and flexural strength of the aggregate while keeping the texture of the aggregate the same. A linear fit to the parabolic equation yielded the "optimal angularity" for basalt and limestone at gradient angles of 3100 and 3137 and the "optimal sphericity" for basalt and limestone at sphericity of 0.68 and 0.63. There is a possibility for future studies to consider controlling the shape or angularity of the aggregates to be the same. In turn, the effect of their texture indices on the different properties of the aggregates will be investigated.

Good surface texture helps to improve the skid resistance of aggregates. However, surface texture belongs to the sub-microscopic category, which is difficult to determine accurately and is mostly replaced by the friction coefficient [94]. The pavement micro-texture is mainly influenced by the aggregate properties inside the pavement. Li et al. [95] characterized the surface texture of aggregates by mean profile depth (MPD) and investigated the relationship between pavement skid resistance and aggregate texture characteristics through extensive experiments and analysis of multiple variables. Zhang et al. [96] proposed an improved pavement texture image segmentation algorithm to comprehensively evaluate the distribution uniformity of asphalt pavement aggregates. The proposed uniformity index (D) of aggregate distribution based on the number and location of texture structures has a good correlation with the texture depth.

Surface textures have mostly been used to study the relationship between aggregates and skid resistance in asphalt paving. For asphalt pavement texture structure distribu-

tion features, field-based visual inspection methods are normally used. This approach is subjective and does not provide a satisfactory assessment of the degree of superiority of the texture structure distribution on asphalt pavement surfaces. DIP techniques are constantly being innovated and applied to study the effect of aggregate morphological features on the performance of road aggregates. Nevertheless, it is difficult to represent the spatial distribution of texture features of road aggregates in 2D images. Attempts have been made to apply 2D image processing techniques to explore texture structure distributions. Regrettably, there is no excellent method to date for determining the state of the texture structure distribution on asphalt surfaces.

In conclusion, 2D aggregate image measurement methods are widely employed in various aspects such as aggregate morphological characteristics, aggregate movement characteristics, void distribution characteristics, etc. By obtaining images of aggregate particles and processing and analyzing the images, the physical properties of aggregates can be studied. Despite the better efficiency of 2D image processing, nonetheless, the vertical depth of 2D image recognition barely reflects the surface texture and spatial morphological features of the aggregates. Meanwhile, since the mixture is a non-homogeneous spatial structure, the interaction between the aggregates and the 2D planar mechanics issue has a large gap.

3.3. Digital Modelling Reconstruction Technology

The microscopic scale properties of aggregated particles have an influential effect on their mechanical properties. In order to further investigate the microscopic scale properties and their macroscopic counterparts, the connection between the above two aspects can be facilitated by 3D digital model reconstruction techniques.

In contrast to the established 2D model, the 3D morphological characteristics of the aggregates are more abundant. In combination with characteristic parameters such as shape and angularity, the 3D aggregate has indicators such as surface texture and roughness, which makes the mechanical behavior of the contact interface more complex. In addition, the extension of 3D spatial coordinates makes the anisotropy of the aggregate accumulation behavior more significant, and the distribution characteristics, such as opening, closing, and connecting of voids, are difficult to predict. X-ray CT, a completely nondestructive technique, allows visualization of the features inside opaque solid objects to obtain digital information on 3D geometric shapes and properties.

Xing et al. [97] investigated the damaging effect of asphalt mixtures on microstructure and aggregate contact based on X-ray CT imaging and DIP methods and analyzed the relationship between the damage factor and contact properties. The results showed that there is a strong linear relationship between the distance of the main skeleton aggregate and the breakage factor [98]. Kutay et al. [69] developed algorithms to calculate the aggregates' size, location, contact points and orientation, which is an excellent solution for better acquisition of microscopic images of aggregates based on the X-ray CT technique. The main representations are the segmentation of close aggregates and processing noisy or poorly contrasted images. The proposed image processing algorithm can guarantee the accuracy of acquisition and recognition by over 95%. Moreover, their findings also indicate that the number of contact points increases significantly with increasing compaction level and direction.

You et al. [99] proposed a framework that can be used to simulate the microscopic response of asphalt mixtures under various loading conditions. Identifying the microstructural composition of asphalt mixtures by X-ray CT imaging and other image processing techniques, the 3D microstructure of asphalt mixtures was obtained and converted into a finite element model to describe its mechanical behavior. The models in their findings reflect the effects of temperature, loading rate, repeated loading and mix ratio design on the microstructure response. Thus, macroscopic design specifications for aggregates can be achieved and guided by X-ray CT-based microscopic modeling methods.

Tashman [100] used an X-ray CT system and image analysis techniques to analyze the pore distribution in asphalt concrete specimens. During Superpave gyratory compaction, when the number of gyrations increased from 50 to 174, the void fraction distributed in the top and bottom regions also increased from 65% to 80%. The distribution of void fractions may be due to the presence of some factor that weakens the compaction effect in the top and bottom regions. The gyratory compactor's top and bottom regions can restrict the aggregate's flow.

Alterations in temperature can also lead to changes in the compaction characteristics of the specimens, which can affect the roadworthiness of the aggregates. Zhang et al. [101] tested the compaction levels of asphalt mixture specimens (AC13, AC16 AC20, and SMA13) under different compaction parameters at different temperatures and obtained high-quality images based on X-ray CT imaging for the microstructural characterization of asphalt mixtures. Variations in the size of the aggregates at the same temperature condition affect the compaction properties. The smaller the particle size, the higher the level of compaction. The larger the particle size, the larger the effect of temperature on the compaction level of the mixture. Figure 7 shows 3D curved surface plots of the variation in compaction level for the AC16 mixtures with an increasing gyration number for three different temperature conditions. However, the conclusions of their study were affected by the morphological characteristics of the aggregates. Therefore, variations in the parameters of the morphological characteristics of aggregates should be taken into account in subsequent studies to draw more general conclusions.

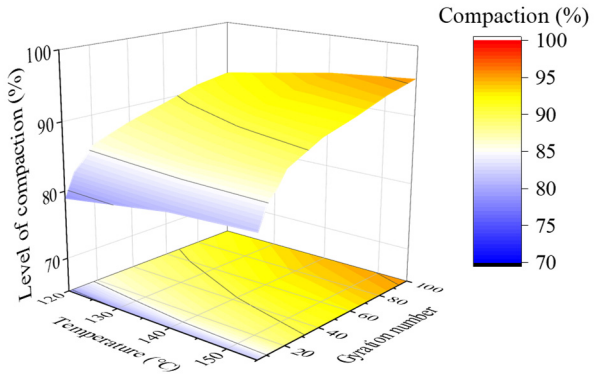

Figure 7. Surface plots of the variation in compaction level versus gyration number for the AC16.

Undoubtedly, high-temperature deformation of asphalt mixtures is a key research direction for asphalt pavement damage. The critical issue in this area concerns the accurate assessment of the effect of aggregate microstructure on the high-temperature deformation of asphalt mixtures. Hu et al. [102] used X-ray CT data to establish the internal microstructure and used DIP techniques to process the 3D model. An adaptive threshold segmentation algorithm based on the annular region was improved and used to extract aggregates and air voids from the gray-scale images. The morphological distribution of pores and aggregates was also determined. The high-temperature damage mechanism of asphalt mixtures was effectively investigated.

The air-void areas in the range of 0–20 mm are reduced to a greater extent by the compression of the load. At the same time, the voids expand into macroscopic cracks in the range of 20–50 mm. At high-temperature deformation, the modification of the air voids is considerably affected by the size and content of the aggregates. This confirms that the study of the morphological characteristics of the aggregates is essential, in particular, to analyze the macroscopic properties of the aggregates. In addition, the results of the study indicate that the motion of the aggregates causes the failure of the asphalt mixture.

Future work should focus on the effect of the morphological characteristics of aggregates on their motional properties and then investigate the effect of changes in morpho-

logical characteristics on the performance of road aggregates when the aggregates move during high-temperature deformation.

To investigate the influence of the morphological characteristics of aggregates and the distribution of air voids on the mechanical properties and performance of asphalt concrete and then to investigate the mechanism of microstructural changes in the aggregate. In a subsequent study, Hu et al. [103] used an X-ray CT device to scan the internal microstructure of typical asphalt concrete and used DIP techniques to study the microstructural changes before and after high-temperature damage. An adaptive threshold segmentation algorithm based on image radius was proposed, which was applied to obtain binary images of aggregates, air voids and asphalt mastic. This method effectively distinguishes the target from the background. The distribution of air voids in asphalt mixtures is obviously affected by their gradation and coarse aggregate size. It was concluded that the aggregate shape could affect the RA. Additionally, the maximum value of RA was reached when the SF of the aggregate particles was taken to be between 1.5–3.5.

Hence, it can be seen that X-ray CT images, as well as digital model reconstruction techniques, can correlate the gradation design and microstructure of aggregates with macroscopic properties.

In general, the introduction of the AIMS system and X-ray CT technology provides great convenience for studying the morphological characteristics of aggregates, and the 3D digital reconstruction technology can better study the microstructural characteristics of asphalt mixtures. At present, most studies mainly use 2D digital image reconstruction and industrial X-ray CT scanning to establish and characterize the 3D morphological model of real aggregates. 2D image processing methods are more efficient in a generation but difficult to describe the surface texture of aggregates finely, while industrial X-ray CT equipment is expensive and has complicated algorithm requirements.

4. Numerical Simulations and Modeling Based on Visualization Techniques

As an important branch of road material design, the accuracy and reliability of the mesoscopic modeling design method depend on the precision of the aggregate visualization technique. Aggregate visualization techniques and mesostructure modeling provide significant solutions to the study of the strength mechanisms of pavement materials. An example is the material genome study of asphalt concrete. However, there are numerous limitations in meso-mechanical numerical modeling due to the available computer technology and hardware facilities. For example, refined aggregate modeling requires a large amount of memory, and the computation of contacts between irregular aggregates is complicated and consumes a large amount of computational time. These reasons make aggregate visualization techniques necessary to be compatible with the reliability of numerical models. Thus, this section briefly introduces numerical modeling methods related to aggregate visualization.

In numerical modeling, idealized numerical modeling is widely used [104]. Two main types of modeling are distinguished: modeling related to metrological properties and modeling related to morphological characteristics. The main difference lies in the choice of regular spherical and irregular shapes. In addition, several novel modeling approaches (LDPM, mesoscale modelling) could improve the accuracy and computational efficiency. The illustration of the aggregate modelling categories is shown in Figure 8.

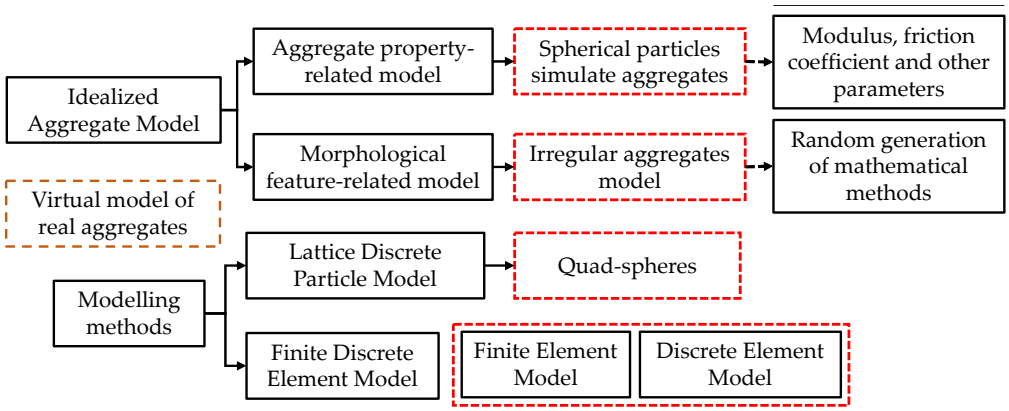

Figure 8. Categories of idealized model and modelling methods for aggregate.

4.1. Idealized Aggregate Model

The self-defined aggregate models can be divided into idealized aggregate models, ordinary angular aggregate models, and special angular aggregate models. This chapter focuses on and summarizes the self-defined digital aggregate models. The previous article describes in detail the application of X-ray CT-based imaging technology. The digital aggregate modeling approach based on aggregate properties is shown in Figure 9.

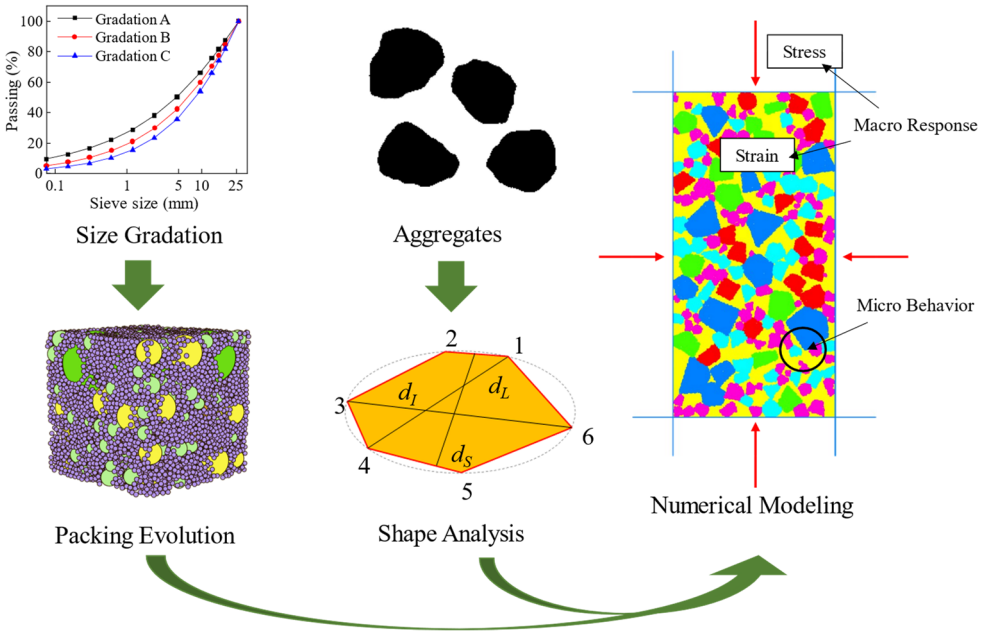

Figure 9. Digital aggregate modeling approach based on aggregate properties.

Existing research tends to combine aggregate accumulations with computer computing to deal with the complex problems arising from the accumulation of large numbers of particles by modeling the dense accumulation of particle assemblies and developing algorithms. Liu [105] used the discrete element method to simulate the creep flexibility tests of ideal HMA mixtures. A total of 102 digital specimens of ideal asphalt mixtures were constructed by two user-defined models, and both the DE model and the FE model are capable of building ideal models. Tan [106] developed a finite element model of an aggregate consisting of multiple randomly distributed irregular aggregates and cement mortar, which was also used to calculate the effect of large-size recycled coarse aggregate on the strength of recycled aggregate concrete. Kurumatani [107] proposed an isotropic damage model for quasi-brittle materials and demonstrated its performance in the anal-

ysis of crack extension in concrete. A benchmark test of a mixed-mode fracture was also performed to demonstrate the performance of the proposed damage model. A simple and reliable two-dimensional finite element (FE) model was defined by Bencardino [108]. The comparison between numerical analysis results and experimental data was also used to highlight the reliability of the finite element model and analytical model.

Structural indicators of asphalt mixtures determine the mixture's non-uniform nature, which significantly impacts the micromechanical response of the mixture. Virtual modeling based on real aggregates aims to simulate the microstructure of the mixture using computer image processing techniques to extract real aggregates using CT [109,110] or laser scanning equipment. However, Jin et al. [87] proposed a virtual design method for mixture microstructure based on the structural indicators of a digital library of real aggregates, and the microstructure of the virtual mixture was obtained by compaction simulation with DEM software. The microstructure of the virtual mix was obtained by determining the location orientation according to the distribution of the selected aggregates, and the indirect tensile test was simulated numerically to obtain the different mechanical properties of the specimens. Liu et al. [111] proposed a user-defined material model in DEM based on a random polygon algorithm for simulating the dynamic modulus test of asphalt mixes by creating polygon particles to represent the shape and size of aggregates. Meanwhile, Liu et al. [112] developed a 3D visualization simulation technique for random particle generation without the use of the X-ray CT technique and used a 3D discrete cell model to visualize and simulate the microscopic properties of asphalt concrete under mechanical loading.

Most researchers used digital imaging techniques to prepare the required samples. However, this method was laboratory dependent and required the preparation and scanning of real asphalt mixtures to obtain digital samples [113], and expensive equipment, labor consumption, and time costs were limitations, which made it difficult to obtain a large number of numerical samples of different grading types, aggregate shapes, angles, and void ratios. Instead, the aggregate stochastic generation model is a method that is independent of the laboratory. The pros and cons of the image-based model and the computer-generated model are summarized and shown in Table 6.

Table 6. Pros and cons of image-based and computer-generated models.

Approach	Pros	Cons
Image = based model	Better accuracy of the real morphology of the aggregates and the internal structure of the composite.	High time cost; Scanning equipment requirement; Limited accuracy of the model; Difficulties with aggregate size and aggregate segregation in 3D schemes.
Computer-generated model	Low cost; No equipment limitations; Undifferentiated aggregates; Facilitates control of aggregate size.	Shape and distribution for aggregate and air voids may not be consistent with the actual condition.

In general, the main advantage of image-based models is the accuracy of the internal structure of the composite, while the main advantage of custom aggregate models is the cost-effectiveness and ease of implementation of the model [114].

Stochastic numerical modeling, a new technique developed in recent years, has been used to study the accumulation model and complex rock structure from a probabilistic point of view, which is of great significance in studying the complex problems existing in the accumulation. The stochastic numerical simulation technique generates the spatial distribution form of aggregates and enables the study of aggregate gradation, particle size, particle shape, and porosity.

4.2. Realistic Aggregate Model

Real shape modeling approximates the real aggregate shape by using different particles, which is especially needed in DE models [115]. Numerical models based on real aggregate models can save time and material, which is much better than the numerical models obtained by X-ray imaging techniques because numerical aggregate particles can be stored and reused to reconstruct the numerical model of the aggregate.

Since the 3D structure of aggregates cannot be clearly visualized, Wang [116] used a method for the automatic generation of spherical clusters to model the 3D shape of real aggregates. Latham [117] built a realistic aggregate model based on laser scans of the aggregate surface from different angles. A 3D meshing of the aggregate particles was performed for finite element modeling, which was further investigated by creating a shape library. In many previous studies [118], non-overlapping circular clusters were utilized to represent the true shape of irregular aggregate particles, which indicates that the nature of the real aggregate model is using small circles or spheres to simulate the real shape of aggregate particles. An example of the randomly generated aggregate basic unit is shown in Figure 10. In the figure, the red extension line indicates the direction of the long axis of the irregular particle cluster clump.

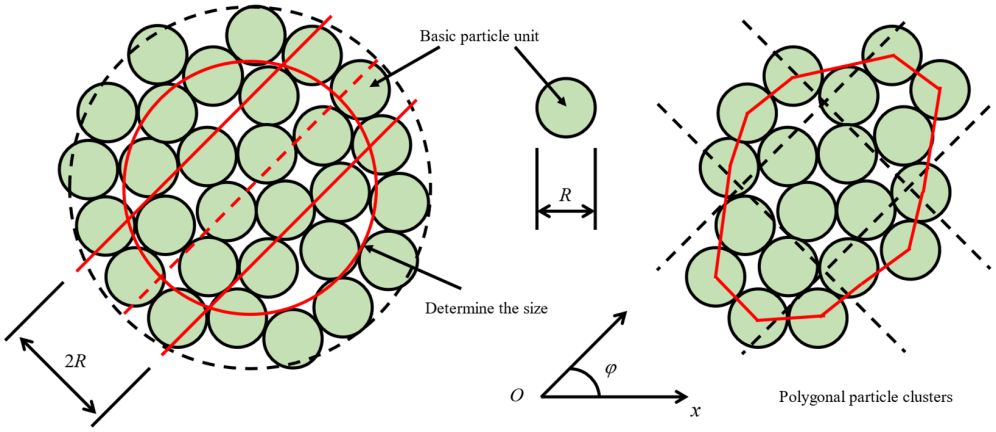

Figure 10. Basic unit and polygon particle clusters.

Sobolev et al. [119] developed an algorithm for simulating the dense accumulation of large, spherical materials and investigated the way of particle filling and particle distribution by geometrical parameters and model variables. Gopalakrishnan et al. [120] applied the concept of particle stacking simulation to develop a model of stable random dense stacking of particles with size distribution and studied the density and coordination number of fillers. Combined with nondestructive imaging and DEM simulation techniques, various parameters of the aggregate structure were optimally described. Fu et al. [121] proposed a novel computer simulation of random stacking of variable-size particles in 3D space using DEM to model particle matrix stacking. Liu et al. [122] used ellipsoidal and convex polyhedral particle random stacking models to study the effect of aggregate shape on the 3D diffusivity of mortar. The diffusivity of mortar was predicted by combining numerical fine view structure and dot matrix methods. The results show that aggregate shape has a significant effect on mortar diffusivity. He et al. [123] utilized DEM to develop a novel system that can consider particle size, shape and filling method and proposed a numerical calculation method for dynamic motion calculation. The results showed a significant effect on filling density by particle shape. Salemi et al. [71] proposed a method for mixing image scanning with aggregate filling to randomly generated 2D digital asphalt concrete specimens for virtual testing and captured the detailed shape characteristics of the aggregates by calibrated high-resolution images. The differences between the simulated results and the measured values are discussed. Du et al. [124] proposed a practical modeling method for 2D arbitrarily shaped aggregates. An effective algorithm is proposed

for large-volume concrete with aggregate content up to 60–70%. The effect of aggregate shape on the mechanical properties of concrete was analyzed and explored. Ma et al. [125] demonstrated in detail a convex extension method for constructing convex polygons and polyhedral represented by crushed coarse aggregates in two and three dimensions by building a fine-scale structural model of three-phase, fully graded concrete consisting of anisotropic high-content aggregates and cement slurry. Li et al. [126] introduced a method for constructing convex extensions using parametric shape and particle size gradation for the simulation of aggregates and asphalt mixtures and used plane geometry factor (PGF) and section aspect ratio (SAR) to describe the 3D geometric characteristics of aggregates. A simplified method of asphalt mortar filling based on a coarse aggregate skeleton is proposed to obtain a dense structure of asphalt mixtures. A digital specimen of asphalt mixtures is shown in Figure 11.

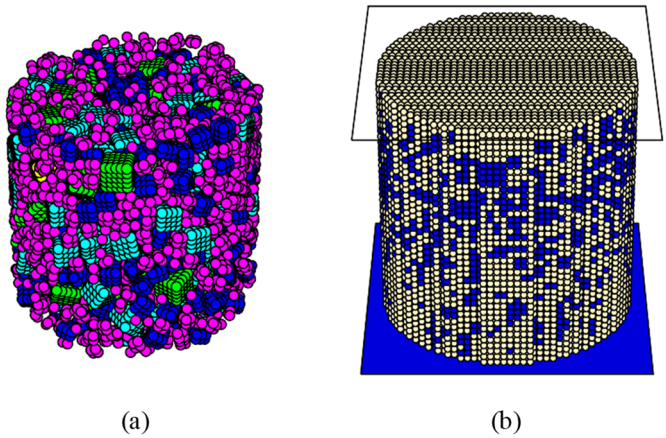

(a) (b)

Figure 11. Digital specimen of asphalt mixtures: (a) aggregate skeleton; (b) specimen assembly.

Modeling real aggregated shapes using ball clustering or clumps requires a balance between modeling accuracy and the number of balls [127]. In other words, the more balls, the more accurate the model, and the longer the computation time, inspiring the users.

4.3. Numerical Methods

The two main types of numerical simulation methods are the DEM method and the Finite Element Method (FEM). Both methods have been mentioned several times in this manuscript, and their applications to numerical reconstruction models have been reviewed. In addition, two novel models, namely LDPM and mesoscale modelling, are introduced in this section.

Meso-structure modeling methods are effective tools for understanding the mechanical behavior of stone-based materials and provide an important complement to experiments. Yang [128] reconstructed the fine-structure model of stone matrix materials by building a library of realistic shape-based numerical representations of aggregates with high accuracy and time and cost savings for both discrete and finite element models. Zhou et al. [129] developed a full 3D mesoscopic finite element model of concrete and used an advanced finite element mesh solver to mesh the highly unstructured region. The 3D mesoscopic numerical simulations were performed on concrete specimens under different loading conditions. Yu [130] performed 2D multiphase simulations of recycled aggregate concrete using the interface element technique to investigate the relative strength of old and new mortar, the amount of bond of old mortar, the performance of the transition zone between old and new interface, and the replacement rate of recycled aggregate. Coleri [131] developed 2D and 3D micromechanical finite element models by ABAQUS, which has strong nonlinear functions. Liu [126] investigated the shear modulus of steel-reinforced recycled aggregate to solve the problem of difficult interface modeling in finite element analysis that does not allow for a proper and accurate consideration of the bonding properties. Souza [132]

conducted uniaxial static creep tests and indirect tensile fracture energy tests and combined the fracture energy test results with finite element simulations of virtual specimens to investigate the effect of the angle of the aggregate prism on the properties and characteristics of the mix. Shahbeyk [133] used FEM to simulate a two-phase cubic concrete specimen containing spherical aggregates in homogeneous mortar, studied the damage of concrete from a fine viewpoint, and investigated the damage of concrete. Wang [134] proposed a random aggregate structure generation method for round and angular aggregates based on the Monte Carlo random sampling principle, which was combined with nonlinear FEM for a fine-view concrete study. Liu [47] developed 3D finite element models for different aggregate angles by keeping other properties of asphalt mixes constant and artificially reducing the angle of aggregates, and uniaxial compression test simulations were carried out. The relationship between the angle of the aggregate prism and the mechanical response of the asphalt mixture in terms of bearing capacity, asphalt mastic creep deformation, damage behavior and energy dissipation were investigated. The calculation results showed that the aggregate angle of inclination had a significant effect on the mechanical properties.

The major theories of DEM [135] are derived from molecular dynamics and particle media mechanics, also known earlier as the particle element method, and proposed by Cundall to analyze the stacking behavior of bulk particles, which is considered to be a unique advantage in dealing with the fine-scale mechanisms such as displacement, rotation and contact fracture of granular materials [136]. The compaction of asphalt mixtures is actually a process of aggregate accumulation in which slip occurs between the aggregates [137]. Therefore, DEM can simulate the compaction process of the asphalt mixture. Figure 12 presents the transformation of the aggregate from images into discrete element models. Figure 13 is a flowchart of the DEM modeling of asphalt mixtures considering composition and structural characteristics.

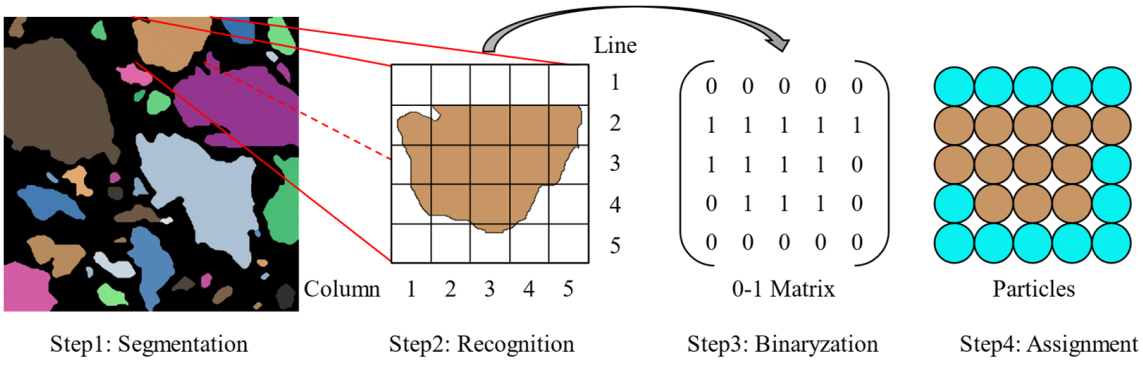

Figure 12. Transformation of the aggregate from images into discrete element models.

At present, the general and technically mature discrete element software includes PFC, a commercial granular flow software developed by Itasca; MatDEM, a matrix discrete element software independently developed by Nanjing University; Yade, a large open-source discrete element software, and SudoDEM.

The investigation of morphological characteristics allows for a better understanding of the mechanical behavior of aggregate particles. The volume or mass of the stone base material is composed of mineral aggregate particles, whose morphological characteristics allow the creation of a digital sample and a discrete element modeling [138]. Collop et al. [139] used an artificially generated specimen of an idealized asphalt mixture. The behavior of a highly idealized asphalt mixture was simulated by different unit models in uniaxial compression creep tests. Meanwhile, Collop et al. [140] investigated discrete unit models to simulate the behavior of highly idealized asphalt mixtures under uniaxial and triaxial compression creep tests, which used single-size spherical particles to model mineral aggregates and the highly ideal model to simulate the expansion and deformation of the asphalt mixture; however, the models were clearly not accurate enough in representing

the shape of the aggregates. Asphalt concrete or cement concrete mixtures were simulated by scanning laboratory-prepared samples, processing the images, and reconstructing the microstructure through image pixels. You et al. [141] developed a microstructure-based 3D discrete unit model of asphalt mixtures to study the dynamic modulus in stress-strain response under compressive loading. The 3D model predicted better than the 2D model. The effect of different void fractions and aggregate modulus on the modulus of the mix was significant.

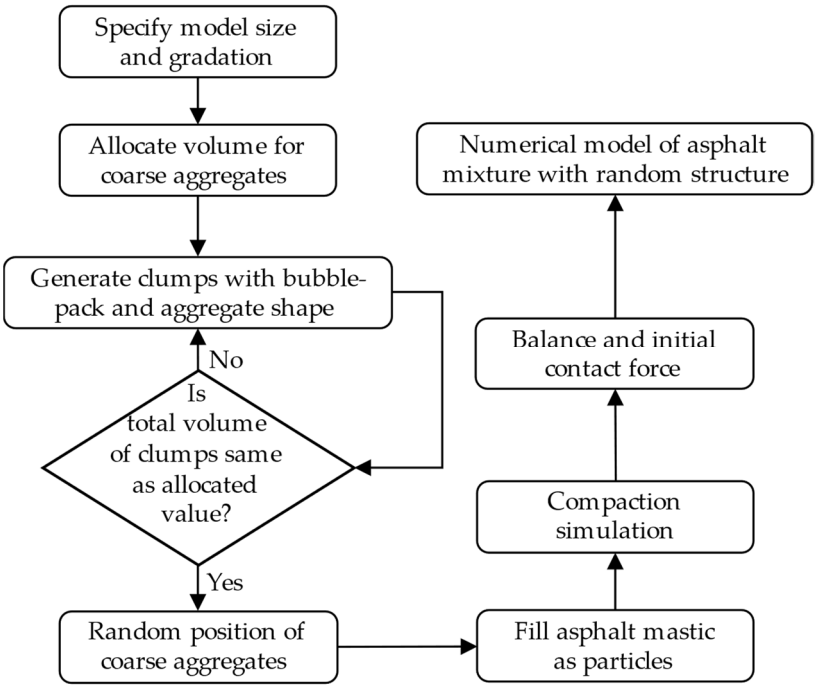

Figure 13. Flowchart of DEM modeling of asphalt mixtures.

Wang [142] developed a computationally efficient DEM method that directly employs spherical harmonic functions to simulate 3D irregularly shaped particles. Dondi et al. [143] used the 3D discrete element method to study the combined effect of aggregate particle shape and angle on the accumulation and stability of the aggregate in asphalt mixtures, and conducted triaxial tests on different types of particle specimens and obtained the results when the shape and angle of the particles had a significant effect on their properties. Ferellec et al. [144] used overlapping spheres to establish a DEM of irregular particle shapes and discussed the effect of parameters on particle shape resolution. Fu et al. [145] used DEM to study the effect of particle shape on the shear localization of granular materials. He et al. [146] used a parallel algorithm-based DEM system to simulate aggregate and cement structures. Zhang et al. [147] developed an algorithm for generating 3D aggregates and used the discrete cell model generated by the algorithm to predict the mixing modulus in different loading frequency ranges. Yao et al. [148] used DEM to numerically simulate asphalt concrete specimens, considering coarse recycled aggregates' distribution characteristics. The results showed that temperature and loading rate significantly affect the damage strength. Meanwhile, Yao [149] investigated the differences in mesoscale characteristics between irregularly shaped and proportioned the soil-rock mixture (SRM) models using the discrete element method, which can accurately predict the mechanical properties and deformation behavior of SRM. The pros and cons of FEM and DEM are summarized in Table 7.

Table 7. Pros and cons of FEM and DEM.

Methods	Pros	Cons
FEM	(1) Accurately model the micro geometry of aggregates and asphalt. (2) Investigate the internal strain distribution of asphalt mixes.	(1) Inability to solve the issue of aggregate-to-aggregate sliding in asphalt mixes, which makes the geometrical characteristics of aggregate contact not change dynamically. (2) Inherent defects in dealing with large deformation problems such as fracture behavior of microstructures. (3) The characteristics of voids in asphalt mixtures have not been fully considered.
DEM	(1) Better characterization of the microstructure of asphalt mixes. (2) Convenient to simulate large deformation mechanical behavior such as cracking.	(1) The time step in the calculation needs to be small, and the number of cells is large, and the computational efficiency needs to be improved (2) The linkage between aggregate distribution state and macroscopic mechanical properties has not been clearly established. (3) The mechanism of the influence of the aggregate distribution state on the properties of asphalt mixtures is not revealed.

Sherzer [150] proposed a novel model to obtain quad-sphere discretization in candidate aggregate spheres, thus enabling the introduction of local discussions around selected aggregate spheres. The introduction of four smaller spheres can replace the original aggregated sphere, and experimental tests show a better fit and a straighter cracking pattern for this method, indicating a more brittle behavior. Sherzer [151] investigated the structural response of concrete under different loads using LDPM in comparison with FDEM. Simulations of uniaxial compressive strength, Brazilian disk and three-point bending were also performed using these two methods, respectively. Obtaining the size effect contributes to the accuracy of the prediction of the structural response and properties of the aggregate.

Naderi [152] proposed a mesoscale model, considering the structural properties of concrete to study the fracture process of concrete under uniaxial and biaxial compression tests. The irregularity of the aggregates is an important factor in the fracture of concrete. His results showed that the compressive strength of concrete is significantly affected by the random position and size distribution of aggregates. However, the shape characteristics of the aggregates do not have much influence, suggesting that simplified aggregate shapes can be used to predict their compressive strength.

Finite elements can establish the connection between the microscopic material and the macroscopic mechanics of the structure. Nevertheless, apart from the real microstructure, the accuracy of mechanical response depends more on the complexity and convergence of the intrinsic model. However, the discrete element method is based on the principle of discontinuous medium mechanics, which bypasses complex mathematical expressions and parameter take-offs. It can fundamentally establish the connection between the microscopic properties of aggregates and the mechanical properties of the mixtures.

5. Applications and Outlook

Gradation measurement is important for quality control of pavement construction. The gradation is obtained by digital image segmentation of the aggregates and transformed from 2D to 3D gradation. The visualization studies of the morphological characteristics of aggregates, as seen in the void fraction and gradation design of aggregates, include the development of 2D images and 3D digital reconstruction techniques for better application in engineering practice [153]. The mechanical properties and dimensional effects analysis of different aggregates are discussed through the establishment of real aggregate models and stochastic models.

5.1. Aggregate Void Ratio and Gradation Design

Asphalt mixtures are multiphase composites consisting of asphalt binder, coarse aggregate, fine aggregate, mineral filler and other additives. The properties of asphalt mixtures are closely related to the volume fraction and spatial distribution of these components. The void fraction is one of the important volumetric properties that affect the stability and durability of asphalt mixtures [154]. Dubois et al. [155] quantified the inhomogeneity of pore distribution by measuring the internal structure of rotating compacted specimens and roller compacted specimens with gamma rays.

X-ray CT and image analysis techniques allow non-destructive and accurate analysis of void distribution in asphalt mixtures. Liu et al. [156] applied DIP techniques based on X-ray CT technology to reconstruct the 3D microstructure of asphalt specimens and determine the specimen tensile strength. During the compaction process, the 3D fractal dimension of the pores showed a trend of first changing and then changing. A hypothesis based on the evolution of the 3D fractal dimension of the pores is proposed to explain the phenomenon.

Park et al. [157] evaluated the physical and mechanical properties and sound absorption characteristics of porous concrete by evaluating the design based on the target void ratio and recycled aggregate content and found that the difference between the target void ratio and the measured void ratio was less than 1.7%. Aliha et al. [158] performed a statistical analysis of tensile cracking in asphalt mixes based on the Weibull model to test the void ratio for different parameters. The study results found that the average fracture toughness values and the Weibull parameter decreased by increasing the porosity content.

Mineral gradation is the main factor affecting the road performance of asphalt mixtures, and gradation is one of the important characteristics of the mix. Golalipour et al. [159] studied the effect of aggregate gradation variation on the rutting characteristics of asphalt concrete mixes. Elliott et al. [160] conducted experiments on six asphalt concrete mixes and tested their different gradations to study the effect of gradation variation on the properties of the mixes.

As shown above, the void ratio and gradation characteristics of aggregates often affect their road performance. By visualizing the morphological characteristics of the aggregates, the researchers quantified the internal structure and spatial distribution of the aggregates and investigated the mechanisms affecting the road performance of the aggregates. The iterative revision of the research results has effectively improved aggregate performance.

5.2. Compaction Method of Aggregate Specimens

The application of different compaction techniques and compaction environments to aggregate specimens may vary considerably. The performance of asphalt mixes is greatly influenced by the quality of the compaction [48]. Excessive or premature permanent deformation and deterioration damage are often the results of inadequate compaction. Commonly used laboratory compaction methods include SGC, vibratory compaction, and plane compaction [92]. Hunter [161] et al. used SGC compaction, vibratory compaction, and field compaction to investigate the mechanical properties of asphalt mixtures from stiffness, modulus, permanent deformation, and fatigue resistance after compaction. The results showed that the mechanical properties were not the same after the same degree of compaction.

The Marshall impact compaction method [162], as the first and most widely used method, takes into account volumetric parameters as well as Marshall stability and flow rate, etc. The SGC method is usually [163] used for testing purposes such as analyzing volumetric properties of asphalt mixtures, evaluating mixture denseness, estimating sensitivity to aggregate shape, and field quality control. Specimens using the SGC method can well simulate the density, aggregate orientation, and structural characteristics of asphalt mixtures on real pavements [109]. Both methods have been used extensively by domestic and international researchers for evaluating and analyzing the performance of asphalt mixtures, and the two methods have been compared to complement each other [164,165].

The purpose of compaction is to reduce a void fraction, optimize aggregate contact behavior and increase bulk-specific gravity [166]. The compositional properties of the asphalt mix, compaction environment, compaction method and field conditions may lead to changes in compaction results. Coenen et al. [167] investigated the development of software that can be used for 2D image analysis and aggregate structure characterization of asphalt mixtures, which has the advantage that the images can be processed prior to the analysis so as not to affect the accuracy of the results. By using the SGC method, the aggregate structure characteristics of the specimens were analyzed under different compaction conditions, including the orientation, spatial distribution, and a number of contact points of the aggregates in the images, and key features describing the influence of the aggregate structure and compaction conditions were proposed. Chang [168] developed a new method to generate 3D models of real aggregate shapes to characterize aggregate segregation during the Superpave gyratory compactor (SGC). In addition, the orientation and distribution of aggregates in asphalt mixtures have an important influence on the performance of asphalt mixtures. Hassan et al. [169] used different compaction methods (gyratory compaction, vibratory compaction and slab compaction) to compact gap-graded asphalt mixture specimens and analyzed the image characteristics using the X-ray CT technique to characterize the orientation and distribution of the ground in the compacted specimens. The results showed that the aggregates near the edge of the samples tended to be arranged along the circumferential direction, while those near the center of the samples were randomly oriented. Figure 14 presents the random asphalt mixture and virtual compaction model.

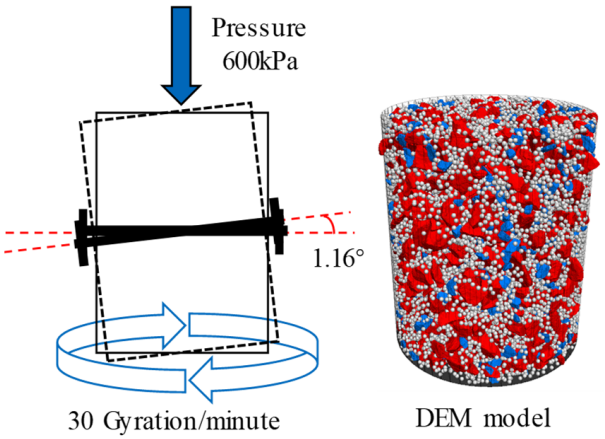

Figure 14. Simulation of asphalt mixtures with SGC.

In summary, scholars have explored the changes in asphalt mixtures under different compaction parameters by varying their relevant properties. Moreover, the existing studies mainly stay in the compaction process without changing the loading parameters. Nevertheless, the loads in the real working environment are adjusted, and how to change the simulated compaction loads at different stages is a problem to be solved in subsequent studies.

5.3. Mechanical Properties and Dimensional Effects of Aggregates

Aggregate shape and spatial distribution influence the microscopic mechanical properties because particle shape and spatial location lead to anisotropy in the interaction between particle skeletons and stress dispersion effects, and this microscopic behavior undergoes redistribution and alternate evolution as new contacts are created and slip during loading.

Aggregates are an important component of cementitious granular materials (CGMs) and significantly impact their mechanical properties. Jiang [170] systematically evaluated several factors affecting the macroscopic compression response of CGMs, including aggregate shape, strain rate, and moisture conditions, with the help of CT focusing on the

corresponding microscopic feedbacks, and combined the aggregate fine-scale fracture mechanics with the macroscopic damage of CGMs to reflect the shape effect of aggregates by quantifying the effect of crushed bricks, whose mechanical properties as coarse aggregates in concrete has been the focus of research [171]. Bektas [172] evaluated the effect of fine aggregates of crushed clay bricks on durability using mortar specimens.

Considering the void ratio of the aggregates as well as the gradation, etc. Mostofinejad [173] used spherical particles to represent aggregates and modeled aggregate filling. The use of spherical aggregates lacked representativeness and realism. Previous studies have used regular spheres to represent aggregates and build aggregate filling models to predict the accumulation density of aggregates. DEM simulations, which randomly generate irregular aggregate models by mathematical methods, do not represent the real shape of the aggregate. Li [174] established a 3D digital model of the real shape of irregular aggregates and concluded that the more irregular the shape of the aggregate, the higher the natural accumulation void ratio. Zhao [175] generated a DEM stacking model to reflect the real shape of the aggregates based on digital photogrammetry. Under external forces, the distribution of particles becomes tighter, and the porosity of the sample becomes smaller. Overall, the stacking density of particles with different elongation index (EI) and flatness index (FI) values increases with the increase of EI and FI values, indicating that flatter or more elongated particles lead to less dense stacking. The results for the packing density are shown in Figure 15.

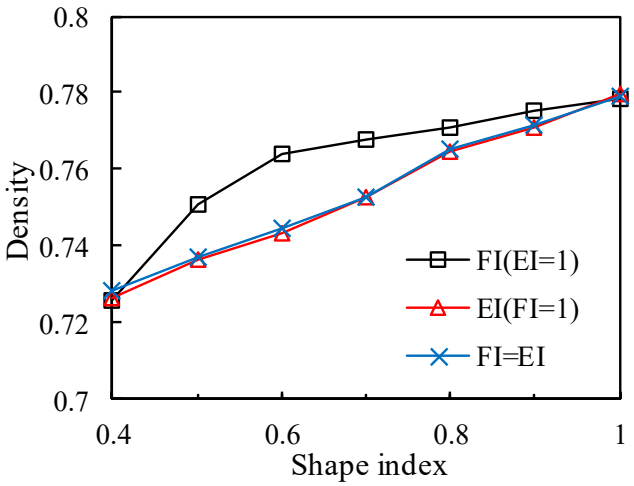

Figure 15. The results for the packing density.

Wu [176] combined DIP and 3D reconstruction techniques to digitize the aggregate morphology and quantitatively analyzed the effect of the spatial distribution of voids in different grades of aggregates. The aggregate loose packing is divided into the top (V_t), middle (V_m) and bottom (V_b). As shown in Figure 16, the packing density gradually increases with the increase of aggregate sphericity or decrease of angularity index (AI) under different gradation conditions.

The strength of concrete is mainly determined by two factors, water-cement ratio and compactness, while the shape of coarse aggregates largely determines the stresses of crack formation. Under increasing loads, the aggregate shape influences concrete fracture energy, tensile strength and modulus of elasticity [177]. Jaya et al. [178] prepared AC14-graded aggregates and evaluated the influence of aggregate shape on asphalt concrete mixes. The effect of cubic aggregates in asphalt mixes can improve their volumetric properties. Increased geometric irregularity of aggregates significantly improves their stability. Sun et al. [179] investigated the effect of aggregate shape on the fine mechanics prediction of viscoelastic properties of asphalt concrete based on random aggregate generation and digital image processing techniques.

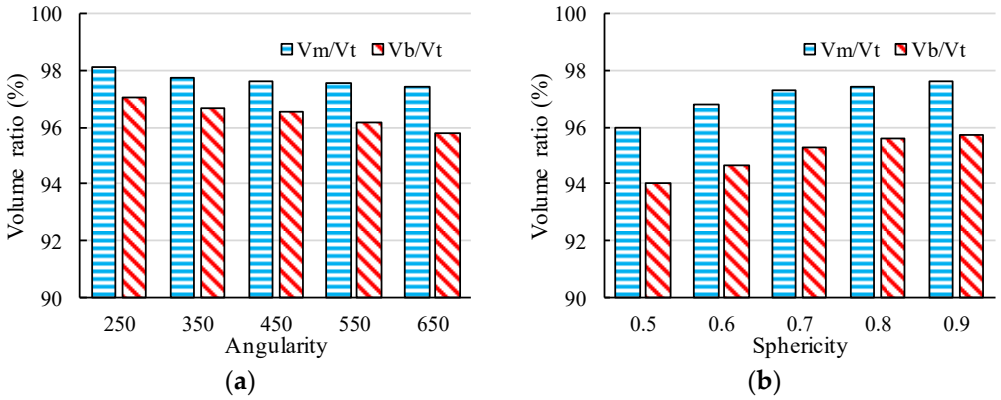

Figure 16. The volume ratio of aggregates at different parts affected by: (**a**) angularity; (**b**) sphericity.

Sengoz et al. [180] investigated the effect of aggregate shape on the surface properties of hot-mix asphalt and evaluated the weaving and friction properties of asphalt mixtures. Lucas Júnior et al. [27] concluded that the mechanical properties of hot mix asphalt are influenced by the properties of aggregates and asphalt binder by studying the shape characteristics and texture of aggregate particles as an indicator of aggregate properties. Pouranian [181] investigated the effect of coarse aggregate shape characteristics on the compaction and microstructural properties of asphalt mixtures using DEM simulations, and among the aggregate shape characteristics parameters, flatness, elongation, roundness and sphericity were statistically correlated with the initial density of the asphalt mixture as a compaction parameter.

Shigang [4] investigated Polyurethane Polymer Concrete (PPC) and analyzed its mechanical properties. The effect of aggregate shape on the mechanical properties (strength, modulus of elasticity, damage behavior) of the new concrete was discussed by establishing a two-dimensional finite element model. Rocco et al. [177] investigated the effect of aggregate shape on the mechanical properties of concrete by designing and testing eight simple cementitious composites and found that the aggregate size significantly affected the fracture energy of crushed and spherical aggregates. Cook et al. [182] investigated the effect of aggregate particle shape on the durability and performance of unbound aggregate bases used in road structures. Singh [183] investigated the effect of aggregate particle size on shape parameters and discussed shape parameter measurements for coarse aggregate (CA) and fine aggregate (FA), and compared the shape parameters using statistical methods. Ghabchi [184] investigated the effect of aggregate shape parameters and gradation on Oklahoma's permeability of commonly used aggregate substrates. The study's results showed that an increase in the uniformity factor and the fines content led to a decrease in permeability. Piotrowska et al. [185] investigated the performance of concrete under high triaxial loading. They used a high-capacity triaxial press to study the shape and composition of coarse aggregates to analyze their effect on concrete.

The inhomogeneous microstructural features are affected by the nonlinear mechanical response. Grigorovitch [186] couples macroscopic and microscopic domains using the embedded unit cell (EUC) homogenization method. The EUC method considers standard periodic boundary conditions and specific boundary conditions around the cell boundary. This method is more accurate and efficient in terms of stress than direct numerical simulations. The particular boundary conditions around the UC are necessary to enforce acyclicity. The inclusions have different corresponding stress levels in different regions under different loads.

Meng [187] proposes a new method for the stochastic model building based on the periodic microstructure of aggregates. The models established when periodic boundary conditions are not considered are subject to certain stochastic errors. Most of the boundary conditions are reflected in the variance of the elastic modulus. It is worth noting that when the model size is very small, the boundary conditions cannot be neglected even

more. The boundary effect and the size effect have significant effects on model accuracy; however, most studies do not consider them. Considering boundary effects when predicting aggregates' tensile or compressive strength can effectively reduce the errors introduced by the calculations. Meng [188] generated a UC that takes into account periodic boundaries to characterize the periodic microstructure of aggregates by an efficient algorithm. The effect of the boundary conditions on the elastic modulus is investigated separately for different size models. Periodic boundary conditions enable the UC model to produce higher elastic moduli. Both the increase in sample size and the increase in UC size reduce the boundary effect. The above studies facilitate the rapid design and optimization of granular materials to increase the aggregate capacity for road use. In the future, multiscale numerical simulations can be performed to investigate more complex material properties.

Asphalt mixtures are a multi-phase system, and the contact parameters of aggregates and asphalt mortar need to be determined separately. Qian et al. [189] investigated the tracking void fraction and distribution of aggregates and asphalt mortar during compaction by establishing an indoor compaction numerical simulation method considering both the critical aggregate particle size and boundary effects and developed a stacking model with binary particle combinations to determine the size limits of fine particles. Alam et al. [190] conducted a three-point bending test for concrete crack openings with similar geometry but different dimensions, combined with digital image processing techniques to observe crack expansion on the specimen surface. They investigated the effect of size effect on crack expansion. Jin [191] established a three-dimensional mesoscale numerical calculation method. It conducted a splitting tensile damage test study on concrete cubic specimens with different lengths, different aggregate contents and maximum aggregate particle sizes. The static and dynamic uniform size effect law can quantitatively predict the size effect of splitting tensile strength of concrete. The size effect is much more pronounced under dynamic than static loading. The compressive strength of the aggregates under dynamic loading is enhanced as the size of the aggregate increases. Consider that at high-strain-rate, the dynamic size effect is minimally affected by the aggregate content. The splitting tensile strength of the concrete is continuously enhanced due to the increased strain rate. Based on ANOVA and Weibull, Wang [192] analyzed the underlying mechanism of dynamical dimensionality reduction in roller-compacted concrete (RCC) materials under impact loading. The dispersion of the stress-strain curves and dynamic increase factors for aggregates at high-strain-rate is more pronounced. The dynamic compressive intensity variance of the specimen deserves to be focused on in subsequent studies.

At high strain rates, there is a correlation between the cracking phenomenon and the morphology of the aggregates. The shape of the aggregate belongs to unnatural angles and flatness. This makes the spherical shape not simulate the irregular morphology of the aggregate and cannot characterize the cracking phenomenon. The existence of interconnected structural features of the angular aggregates in the real specimen model allows for enhanced interlocking effects. This also results in some enhancement of the compressive strength and fracture toughness of the aggregate. The effect of aggregate shape on the strength of the specimens is enhanced at higher strain rates.

Under external loading, stress concentration occurs within the aggregate particles, leading to structural damage. Along with the increase in strain rate, microcracks appear inside the specimen and gradually expand the rupture surface where cross-cracking occurs. The interaction between the particles is usually manifested as angular fragmentation, with the coarse particles breaking into a body of smaller particle size and a series of fine particles. Aggregate-crack interaction increases the stress intensity factor and energy release rate of interfacial cracking, making concrete more susceptible to cracking and damage. In addition, factors such as aggregate location, particle size and external loading affect the stress intensity factor and expansion angle.

In summary, the characteristic parameters of aggregate shape significantly impact the compressive strength and damage behavior of the concrete. The morphological characteristics of the aggregates also have an influential effect on the mechanical properties of asphalt

mixtures, asphalt concrete and concrete. The studies on the effect of aggregate shape on the compressive properties of concrete have mainly focused on quasi-static loading conditions. Further exploration is still needed for the dynamic state of aggregate shape loading.

6. Summary and Recommendations

The morphological characteristics of the aggregates have a significant impact on the properties of the mixtures. Accurately characterization and evaluation are imperative to correlate morphological characteristics with the mixtures. Visualization techniques can help us better capture images or digital images of the aggregates. On this basis, the structural characteristics of the aggregates are further analyzed using digital model reconstruction techniques to establish the link between macroscopic design indicators and microstructures. In this study, the aggregates' morphological characteristics (shape, angularity and texture) are considered for the evaluation method. The optimal way to characterize the morphological characteristics of an aggregate is to consider several evaluation parameters simultaneously. There is also a connection between these evaluation parameters. The calculation methods of aggregate size range and morphological characteristics applicable to three types of digital image acquisition devices (early digital imaging devices, dynamic imaging techniques, and static imaging techniques) are systematically summarized. Furthermore, the advantages and disadvantages of these devices and techniques are collated and included in Tables 4 and 5.

The idealized modeling approach and the realistic aggregate model for aggregates are reviewed separately, explaining where their respective advantages exist. Mainstream numerical modeling methods (FE, DE) have been used in both idealized and general aggregate models. In addition, some novel methods (such as LDPM) are introduced for aggregate particle modeling to study more accurately the fracture behavior of the mixes and their properties. The methods and techniques described above are designed to serve the working performance of road aggregates. Finally, the void ratio and gradation design of the aggregates are considered, and their mechanisms affecting the performance of the aggregates are analyzed. Different perimeter pressures and dynamic loads also change the relevant properties of the aggregate. In addition, dimensional effects and different boundary conditions also change the microstructure of the aggregate. The effects of morphological features are evaluated to account for particular damage processes and deformation patterns of aggregates. Some summaries and recommendations are shown as follows.

(1) A single quantitative measurement of the evaluation parameters (2D or 3D parameters) cannot fully describe the aggregate morphology. 2D image processing methods generate more efficiency, but struggle to finely describe the surface texture of aggregates. The development of digital image acquisition devices has achieved high accuracy of acquisition results. Nevertheless, part of the morphological features was ignored or missed in the imaging process for computational efficiency or to reach an idealized state. This is a future work that needs to be addressed. It is desirable to ensure that the imaging technique is optimized so that the morphological features of the aggregate can be properly characterized. In addition, the choice of evaluation parameters is also crucial for a proper analysis of the performance of the mixture. Furthermore, efficiency improvements should remain an area of focus. Through the study and analysis of digital imaging acquisition methods, future work should focus on using direct measurements to obtain the morphological characteristics of aggregates and to establish some connection between aggregate morphology and mixture properties.

(2) The advantage of 3D digital modeling is that the obtained void fraction is closer to the actual value of the real specimen. In the 3D numerical model of the mixture constructed based on the one-to-one mapping of 3D image pixels to numerical units, there is only a simple binding relationship between the units. The lack of realistic microscopic interface information prevents the effective simulation of various types of behavior of microscopic interfaces, and the simulation scale is enormous. Microstructure modeling, such as 3D digital model reconstruction based on X-ray CT, can be used to model the level of macro-

scopic specimens at different temperatures, loading and morphological characteristics. The reviewed methods are well-suited to help us understand the effect of microstructure on the macroscopic response of aggregates. Subsequent research has focused on improving the acquisition and recognition methods for aggregated digital images. At the same time, there is broad promise in exploring digital image reconstruction techniques that can reflect the characteristics of real aggregates.

(3) Idealized aggregate models are often used in studies that are not affected by aggregate shape. Numerical models related to the morphological characteristics of the aggregates are more reflective of the real aggregate characteristics. It facilitates the study of correlations between the morphological properties of aggregates and the mechanical properties of mixtures. Consequently, combining the respective advantages of digital image technology and computer modeling can effectively improve the efficiency of digital aggregate modeling. The mutual verification of experimental tests and numerical simulations can provide further insight into the microstructure properties of the mixture. This includes an efficient method to address the anisotropy of mechanical behavior induced by specimen compaction, skeleton embedding, aggregate contact and non-uniform distribution.

(4) Numerical simulations at the microscopic scale have been extensively used to investigate the mechanical behavior, such as stress-strain relations, fracture behavior, and fatigue properties of heterogeneous mixtures with aggregates as the substrate. These inhomogeneous mixtures mainly refer to road engineering composites with aggregate particles and binder slurry as constituents, where cement concrete and asphalt mixtures are represented. Therefore, future numerical studies on unbonded granular materials (graded crushed rock) are needed. The shape characteristics and gradation design of the aggregates influence the meso-mechanical properties. Particle shape and spatial position lead to anisotropy in the interplay between particle skeleton and stress dispersion effects. This microscopic behavior alternately redistributes and evolves as new contacts are created and slip during loading. In the case of contact networks, the inhomogeneity of the contact force explains the strong evidence to elucidate that the particle distribution is disordered and anisotropic. Further development of mesoscale fracture models that can take into account aggregate voids and internal friction is needed in the future. The analysis of whether to consider boundary conditions affects the accuracy of the model results. The model's boundary conditions and size need to be considered simultaneously. From the microscopic analysis, the spherical particles are less prone to cracking phenomena compared to the irregular particle model. Irregular particles lead to more severe aggregate damage. For future research, suitable dynamic loads are selected, and mesoscale models are established to study the evolution of specimens under the coupling effect of micromechanics and macroscopic fracture processes. Of course, this also relies on high-resolution CT scanning devices.

Author Contributions: Conceptualization, J.L.; methodology, Y.Y. and K.L.; software, L.W. and Y.T.; validation, K.L.; formal analysis, K.L.; investigation, L.W.; resources, J.L.; data curation, L.W. and Y.T.; writing—original draft preparation, L.W., Y.T. and J.L.; writing—review and editing, L.W. and J.L.; visualization, Y.Y.; supervision, Y.Y.; project administration, Y.Y.; funding acquisition, Y.Y. and J.L. All authors have read and agreed to the published version of the manuscript.

Funding: This research was funded by the National Natural Science Foundation of China, grant number 52208426; Special Financial Aid to the Post-Doctorate Research Project of Chongqing; Open Fund of Key Laboratory of Special Environment Road Engineering of Hunan Province (Changsha University of Science and Technology), grant number kfj210501; the Key Research and Development Program of Hunan Province, grant number 2021SK2050; the Science and Technology Project of the Department of Transportation of Jiangxi Province, grant number 2022H0024.

Data Availability Statement: Not applicable.

Conflicts of Interest: The authors declare no conflict of interest.

References

1. Zhang, J.; Li, C.; Ding, L.; Li, J. Performance evaluation of cement stabilized recycled mixture with recycled concrete aggregate and crushed brick. *Constr. Build. Mater.* **2021**, *296*, 123596. [CrossRef]
2. Sun, Z.; Li, S.; Zhang, J.; Zeng, Y. Adhesion of Bituminous Crack Sealants to Aggregates Using Surface Energy Theory. *J. Mater. Civ. Eng.* **2020**, *32*, 04020299. [CrossRef]
3. Ren, J.L.; Xu, Y.S.; Huang, J.D.; Wang, Y.; Jia, Z.R. Gradation optimization and strength mechanism of aggregate structure considering macroscopic and mesoscopic aggregate mechanical behaviour in porous asphalt mixture. *Constr. Build. Mater.* **2021**, *300*, 124262. [CrossRef]
4. Shigang, A.; Liqun, T.; Yiqi, M.; Yongmao, P.; Yiping, L.; Daining, F. Effect of aggregate distribution and shape on failure behavior of polyurethane polymer concrete under tension. *Comput. Mater. Sci.* **2013**, *67*, 133–139. [CrossRef]
5. Zhang, D.; Hou, S.; Bian, J.; He, L. Investigation of the micro-cracking behavior of asphalt mixtures in the indirect tensile test. *Eng. Fract. Mech.* **2016**, *163*, 416–425. [CrossRef]
6. Caro, S.; Masad, E.; Bhasin, A.; Little, D. Coupled micromechanical model of moisture-induced damage in asphalt mixtures. *J. Mater. Civ. Eng.* **2010**, *22*, 380–388. [CrossRef]
7. Cannone Falchetto, A.; Moon, K.H.; Wistuba, M.P. Microstructural analysis and rheological modeling of asphalt mixtures containing recycled asphalt materials. *Materials* **2014**, *7*, 6254–6280. [CrossRef] [PubMed]
8. Ng, K.; Dai, Q. Numerical investigation of internal frost damage of digital cement paste samples with cohesive zone modeling and SEM microstructure characterization. *Constr. Build. Mater.* **2014**, *50*, 266–275. [CrossRef]
9. Underwood, B.S.; Kim, Y.R. A four phase micro-mechanical model for asphalt mastic modulus. *Mech. Mater.* **2014**, *75*, 13–33. [CrossRef]
10. Sadd, M.H.; Dai, Q. A comparison of micro-mechanical modeling of asphalt materials using finite elements and doublet mechanics. *Mech. Mater.* **2005**, *37*, 641–662. [CrossRef]
11. Al-Rub, R.K.A.; Darabi, M.K.; Little, D.N.; Masad, E.A. A micro-damage healing model that improves prediction of fatigue life in asphalt mixes. *Int. J. Eng. Sci.* **2010**, *48*, 966–990. [CrossRef]
12. Buttlar, W.G.; You, Z. Discrete element modeling of asphalt concrete: Microfabric approach. *Transp. Res. Rec.* **2001**, *1757*, 111–118. [CrossRef]
13. Kennedy, T.W.; Huber, G.A.; Harrigan, E.T.; Cominsky, R.J.; Hughes, C.S.; Von Quintus, H.; Moulthrop, J.S. *Superior Performing Asphalt Pavements (Superpave): The Product of the SHRP Asphalt Research Program*; American Association of State Highway and Transportation Officials: Washington, DC, USA, 1994.
14. Zhang, J.; Li, J.; Yao, Y.; Zheng, J.; Gu, F. Geometric anisotropy modeling and shear behavior evaluation of graded crushed rocks. *Constr. Build. Mater.* **2018**, *183*, 346–355. [CrossRef]
15. Yang, X.; Chen, S.; You, Z. 3D voxel-based approach to quantify aggregate angularity and surface texture. *J. Mater. Civ. Eng.* **2017**, *29*, 04017031. [CrossRef]
16. Zhang, S.; Li, R.; Pei, J. Evaluation methods and indexes of morphological characteristics of coarse aggregates for road materials: A comprehensive review. *J. Traffic Transp. Eng. (Engl. Ed.)* **2019**, *6*, 256–272. [CrossRef]
17. Li, J.; Zhang, J.; Qian, G.; Zheng, J.; Zhang, Y. Three-dimensional simulation of aggregate and asphalt mixture using parameterized shape and size gradation. *J. Mater. Civ. Eng.* **2019**, *31*, 04019004. [CrossRef]
18. Masad, E.; Olcott, D.; White, T.; Tashman, L. Correlation of fine aggregate imaging shape indices with asphalt mixture performance. *Transp. Res. Rec.* **2001**, *1757*, 148–156. [CrossRef]
19. Jun, Y.; Ye, Q. Morphological character of coarse aggregate and its influence on high-temperature shear strength of asphalt mixture. *J. Traffic Transp. Eng.* **2011**, *11*, 17–22.
20. Xiong, Q.; Wang, X.; Zhang, L. Research summary of digital image processing technology on coarse aggregate morphology characteristics. *Subgrade Eng.* **2012**, *1*, 7–10.
21. Wang, H.; Wang, D.; Liu, P.; Hu, J.; Schulze, C.; Oeser, M. Development of morphological properties of road surfacing aggregates during the polishing process. *Int. J. Pavement Eng.* **2017**, *18*, 367–380. [CrossRef]
22. Singh, D.; Zaman, M.; Commuri, S. Comparison of shape parameters for selected coarse aggregates in Oklahoma. *J. Test. Eval.* **2012**, *40*, 409–426. [CrossRef]
23. Wang, L.; Lane, D.S.; Lu, Y.; Druta, C. Portable image analysis system for characterizing aggregate morphology. *Transp. Res. Rec.* **2009**, *2104*, 3–11. [CrossRef]
24. Al Rousan, T.M. *Characterization of Aggregate Shape Properties Using a Computer Automated System*; Texas A&M University: College Station, TX, USA, 2004.
25. Wang, A.; Zhang, Z.; Liu, K.; Xu, H.; Shi, L.; Sun, D. Coral aggregate concrete: Numerical description of physical, chemical and morphological properties of coral aggregate. *Cem. Concr. Compos.* **2019**, *100*, 25–34.
26. Miao, Y.; Yu, W.; Wu, J.; Wang, S.; Wang, L. Feasibility of one side 3-D scanning for characterizing aggregate shape. *Int. J. Pavement Res. Technol.* **2019**, *12*, 197–205. [CrossRef]
27. Lucas Júnior, J.L.; Babadopulos, L.F.; Soares, J.B. Effect of aggregate shape properties and binder's adhesiveness to aggregate on results of compression and tension/compression tests on hot mix asphalt. *Mater. Struct.* **2020**, *53*, 43. [CrossRef]
28. Mora, C.; Kwan, A. Sphericity, shape factor, and convexity measurement of coarse aggregate for concrete using digital image processing. *Cem. Concr. Res.* **2000**, *30*, 351–358. [CrossRef]

29. Al-Rousan, T.; Masad, E.; Tutumluer, E.; Pan, T. Evaluation of image analysis techniques for quantifying aggregate shape characteristics. *Constr. Build. Mater.* **2007**, *21*, 978–990. [CrossRef]
30. Komba, J.J.; Anochie-Boateng, J.K.; van der Merwe Steyn, W. Analytical and laser scanning techniques to determine shape properties of aggregates. *Transp. Res. Rec.* **2013**, *2335*, 60–71. [CrossRef]
31. Anochie-Boateng, J.K.; Komba, J.J.; Mvelase, G.M. Three-dimensional laser scanning technique to quantify aggregate and ballast shape properties. *Constr. Build. Mater.* **2013**, *43*, 389–398. [CrossRef]
32. Pan, T.; Tutumluer, E. Imaging-based direct measurement of aggregate surface area and its application in asphalt mixture design. *Int. J. Pavement Eng.* **2010**, *11*, 415–428. [CrossRef]
33. Tutumluer, E.; Huang, H.; Hashash, Y.; Ghaboussi, J. Discrete element modeling of railroad ballast settlement. In Proceedings of the AREMA Annual Conference, Chicago, IL, USA, 9–12 September 2007.
34. Ge, H.; Sha, A.; Han, Z.; Xiong, X. Three-dimensional characterization of morphology and abrasion decay laws for coarse aggregates. *Constr. Build. Mater.* **2018**, *188*, 58–67. [CrossRef]
35. Wadell, H. Sphericity and roundness of rock particles. *J. Geol.* **1933**, *41*, 310–331. [CrossRef]
36. Mandelbrot, B.B.; Mandelbrot, B.B. *The Fractal Geometry of Nature*; WH Freeman: New York, NY, USA, 1982; Volume 1.
37. Lee, C.; Kramer, T.A. Prediction of three-dimensional fractal dimensions using the two-dimensional properties of fractal aggregates. *Adv. Colloid Interface Sci.* **2004**, *112*, 49–57. [CrossRef] [PubMed]
38. Wang, L.; Wang, X.; Mohammad, L.; Abadie, C. Unified method to quantify aggregate shape angularity and texture using Fourier analysis. *J. Mater. Civ. Eng.* **2005**, *17*, 498–504. [CrossRef]
39. Zhang, D.; Huang, X.; Zhao, Y. Investigation of the shape, size, angularity and surface texture properties of coarse aggregates. *Constr. Build. Mater.* **2012**, *34*, 330–336. [CrossRef]
40. Rajan, B.; Singh, D. Understanding influence of crushers on shape characteristics of fine aggregates based on digital image and conventional techniques. *Constr. Build. Mater.* **2017**, *150*, 833–843. [CrossRef]
41. Sun, W.; Wang, L.; Tutumluer, E. Image analysis technique for aggregate morphology analysis with two-dimensional Fourier transform method. *Transp. Res. Rec.* **2012**, *2267*, 3–13. [CrossRef]
42. Moaveni, M.; Mahmoud, E.; Ortiz, E.M.; Tutumluer, E.; Beshears, S. Use of advanced aggregate imaging systems to evaluate aggregate resistance to breakage, abrasion, and polishing. *Transp. Res. Rec.* **2014**, *2401*, 1–10. [CrossRef]
43. Wang, H.; Wang, C.; Bu, Y.; You, Z.; Yang, X.; Oeser, M. Correlate aggregate angularity characteristics to the skid resistance of asphalt pavement based on image analysis technology. *Constr. Build. Mater.* **2020**, *242*, 118150. [CrossRef]
44. Kuo, C.Y.; Freeman, R.B. Imaging indices for quantification of shape, angularity, and surface texture of aggregates. *Transp. Res. Rec.* **2000**, *1721*, 57–65. [CrossRef]
45. Isa, N.A.M.; Sani, Z.M.; Al-Batah, M.S. Automated Intelligent real-time system for aggregate classification. *Int. J. Miner. Process.* **2011**, *100*, 41–50. [CrossRef]
46. Kuang, D.; Wang, X.; Jiao, Y.; Zhang, B.; Liu, Y.; Chen, H. Influence of angularity and roughness of coarse aggregates on asphalt mixture performance. *Constr. Build. Mater.* **2019**, *200*, 681–686. [CrossRef]
47. Liu, P.; Hu, J.; Wang, D.; Oeser, M.; Alber, S.; Ressel, W.; Falla, G.C. Modelling and evaluation of aggregate morphology on asphalt compression behavior. *Constr. Build. Mater.* **2017**, *133*, 196–208. [CrossRef]
48. Zhu, X.; Qian, G.; Yu, H.; Yao, D.; Shi, C.; Zhang, C. Evaluation of coarse aggregate movement and contact unbalanced force during asphalt mixture compaction process based on discrete element method. *Constr. Build. Mater.* **2022**, *328*, 127004. [CrossRef]
49. Huang, B.; Chen, X.; Shu, X.; Masad, E.; Mahmoud, E. Effects of coarse aggregate angularity and asphalt binder on laboratory-measured permanent deformation properties of HMA. *Int. J. Pavement Eng.* **2009**, *10*, 19–28. [CrossRef]
50. Miller, T.; Swiertz, D.; Tashman, L.; Tabatabaee, N.; Bahia, H.U. Characterization of asphalt pavement surface texture. *Transp. Res. Rec.* **2012**, *2295*, 19–26. [CrossRef]
51. Al-Assi, M.; Kassem, E.; Nielsen, R. Using Close-Range Photogrammetry to Measure Pavement Texture Characteristics and Predict Pavement Friction. *Transp. Res. Rec.* **2020**, *2674*, 794–805. [CrossRef]
52. Khasawneh, M.A.; Shbeeb, N.I.; Al-Omari, A.A. Analytical tool to shorten polishing time based on mean texture depth (MTD) of flexible pavements. *Road Mater. Pavement Des.* **2020**, *21*, 737–756. [CrossRef]
53. Du, Y.; Weng, Z.; Li, F.; Ablat, G.; Wu, D.; Liu, C. A novel approach for pavement texture characterisation using 2D-wavelet decomposition. *Int. J. Pavement Eng.* **2022**, *23*, 1851–1866. [CrossRef]
54. Hu, L.; Yun, D.; Liu, Z.; Du, S.; Zhang, Z.; Bao, Y. Effect of three-dimensional macrotexture characteristics on dynamic frictional coefficient of asphalt pavement surface. *Constr. Build. Mater.* **2016**, *126*, 720–729. [CrossRef]
55. Cui, P.; Xiao, Y.; Yan, B.; Li, M.; Wu, S. Morphological characteristics of aggregates and their influence on the performance of asphalt mixture. *Constr. Build. Mater.* **2018**, *186*, 303–312. [CrossRef]
56. Pan, T.; Tutumluer, E. Evaluation of visual based aggregate shape classifications using the University of Illinois Aggregate Image Analyzer (UIAIA). In *Pavement Mechanics and Performance*; American Society of Civil Engineers: Reston, VA, USA, 2006; pp. 203–211.
57. Singh, D.; Zaman, M.; Commuri, S. Inclusion of aggregate angularity, texture, and form in estimating dynamic modulus of asphalt mixes. *Road Mater. Pavement Des.* **2012**, *13*, 327–344. [CrossRef]
58. Kutay, M.E.; Ozturk, H.I.; Abbas, A.R.; Hu, C. Comparison of 2D and 3D image-based aggregate morphological indices. *Int. J. Pavement Eng.* **2011**, *12*, 421–431. [CrossRef]

59. Chen, J.S.; Hsieh, W.; Liao, M.C. Effect of Coarse Aggregate Shape on Engineering Properties of Stone Mastic Asphalt Applied to Airport Pavements. *Int. J. Pavement Res. Technol.* **2013**, *6*, 595–601.
60. Fletcher, T.; Chandan, C.; Masad, E.; Sivakumar, K. Measurement of aggregate texture and its influence on hot mix asphalt (HMA) permanent deformation. *J. Test. Eval.* **2002**, *30*, 524–531.
61. Maerz, N.H. Technical and computational aspects of the measurement of aggregate shape by digital image analysis. *J. Comput. Civ. Eng.* **2004**, *18*, 10–18. [CrossRef]
62. Bessa, I.S.; Branco, V.T.C.; Soares, J.B.; Neto, J.A.N. Aggregate shape properties and their influence on the behavior of hot-mix asphalt. *J. Mater. Civ. Eng.* **2015**, *27*, 04014212. [CrossRef]
63. Zhang, J.; Ding, L.; Li, F.; Peng, J. Recycled aggregates from construction and demolition wastes as alternative filling materials for highway subgrades in China. *J. Clean. Prod.* **2020**, *255*, 120223. [CrossRef]
64. Aragão, F.T.S.; Pazos, A.R.G.; da Motta, L.M.G.; Kim, Y.R.; do Nascimento, L.A.H. Effects of morphological characteristics of aggregate particles on the mechanical behavior of bituminous paving mixtures. *Constr. Build. Mater.* **2016**, *123*, 444–453. [CrossRef]
65. Wang, H.; Bu, Y.; Wang, Y.; Yang, X.; You, Z. The effect of morphological characteristic of coarse aggregates measured with fractal dimension on asphalt mixture's high-temperature performance. *Adv. Mater. Sci. Eng.* **2016**, *2016*, 6264317. [CrossRef]
66. Puzzo, L.; Loprencipe, G.; Tozzo, C.; D'Andrea, A. Three-dimensional survey method of pavement texture using photographic equipment. *Measurement* **2017**, *111*, 146–157. [CrossRef]
67. Grenfell, J.; Ahmad, N.; Liu, Y.; Apeagyei, A.; Large, D.; Airey, G. Assessing asphalt mixture moisture susceptibility through intrinsic adhesion, bitumen stripping and mechanical damage. *Road Mater. Pavement Des.* **2014**, *15*, 131–152. [CrossRef]
68. Cui, P.; Wu, S.; Xiao, Y.; Wang, F.; Wang, F. Quantitative evaluation of active based adhesion in Aggregate-Asphalt by digital image analysis. *J. Adhes. Sci. Technol.* **2019**, *33*, 1544–1557. [CrossRef]
69. Kutay, M.E.; Arambula, E.; Gibson, N.; Youtcheff, J. Three-dimensional image processing methods to identify and characterise aggregates in compacted asphalt mixtures. *Int. J. Pavement Eng.* **2010**, *11*, 511–528. [CrossRef]
70. Shi, L.; Wang, D.; Jin, C.; Li, B.; Liang, H. Measurement of coarse aggregates movement characteristics within asphalt mixture using digital image processing methods. *Measurement* **2020**, *163*, 107948. [CrossRef]
71. Salemi, M.; Wang, H. Image-aided random aggregate packing for computational modeling of asphalt concrete microstructure. *Constr. Build. Mater.* **2018**, *177*, 467–476. [CrossRef]
72. Barksdale, R.D.; Kemp, M.A.; Sheffield, W.J.; Hubbard, J.L. Measurement of aggregate shape, surface area, and roughness. *Transp. Res. Rec.* **1991**, *1301*, 107–116.
73. Wang, D.; Wang, H.; Bu, Y.; Schulze, C.; Oeser, M. Evaluation of aggregate resistance to wear with Micro-Deval test in combination with aggregate imaging techniques. *Wear* **2015**, *338*, 288–296. [CrossRef]
74. Gong, F.; Liu, Y.; You, Z.; Zhou, X. Characterization and evaluation of morphological features for aggregate in asphalt mixture: A review. *Constr. Build. Mater.* **2021**, *273*, 121989. [CrossRef]
75. Mangulkar, M.; Jamkar, S. Review of particle packing theories used for concrete mix proportioning. *Contrib. Pap.* **2013**, *141*, 1324–1331.
76. Sun, W. Quantification of Morphological Characteristics of Aggregates at Multiple Scales. Ph.D. Thesis, Virginia Tech, Blacksburg, VA, USA, 2015.
77. Maerz, N.H.; Palangio, T.C.; Franklin, J.A. WipFrag image based granulometry system. In *Measurement of Blast Fragmentation*; Routledge: London, UK, 2018; pp. 91–99.
78. Moaveni, M.; Cetin, S.; Brand, A.S.; Dahal, S.; Roesler, J.R.; Tutumluer, E. Machine vision based characterization of particle shape and asphalt coating in Reclaimed Asphalt Pavement. *Transp. Geotech.* **2016**, *6*, 26–37. [CrossRef]
79. Araujo, V.M.; Bessa, I.S.; Branco, V.T.C. Measuring skid resistance of hot mix asphalt using the aggregate image measurement system (AIMS). *Constr. Build. Mater.* **2015**, *98*, 476–481. [CrossRef]
80. Liu, Y.; Sun, W.; Nair, H.; Lane, D.S.; Wang, L. Quantification of aggregate morphologic characteristics with the correlation to uncompacted void content of coarse aggregates in Virginia. *Constr. Build. Mater.* **2016**, *124*, 645–655. [CrossRef]
81. Liu, Y.; Gong, F.; You, Z.; Wang, H. Aggregate morphological characterization with 3D optical scanner versus X-ray computed tomography. *J. Mater. Civ. Eng.* **2018**, *30*, 04017248. [CrossRef]
82. Mahmoud, E.; Gates, L.; Masad, E.; Erdoğan, S.; Garboczi, E. Comprehensive evaluation of AIMS texture, angularity, and dimension measurements. *J. Mater. Civ. Eng.* **2010**, *22*, 369–379. [CrossRef]
83. Rezaei, A.; Masad, E. Experimental-based model for predicting the skid resistance of asphalt pavements. *Int. J. Pavement Eng.* **2013**, *14*, 24–35. [CrossRef]
84. Wang, L.; Sun, W.; Tutumluer, E.; Druta, C. Evaluation of aggregate imaging techniques for quantification of morphological characteristics. *Transp. Res. Rec.* **2013**, *2335*, 39–49. [CrossRef]
85. Wang, H.; Wang, C.; You, Z.; Yang, X.; Huang, Z. Characterising the asphalt concrete fracture performance from X-ray CT Imaging and finite element modelling. *Int. J. Pavement Eng.* **2018**, *19*, 307–318. [CrossRef]
86. Jin, C.; Li, S.; Yang, X. Adaptive three-dimensional aggregate shape fitting and mesh optimization for finite-element modeling. *J. Comput. Civ. Eng.* **2020**, *34*, 04020020. [CrossRef]
87. Jin, C.; Zou, F.; Yang, X.; Liu, K. 3-D virtual design and microstructural modeling of asphalt mixture based on a digital aggregate library. *Comput. Struct.* **2021**, *242*, 106378. [CrossRef]

88. Li, J.; Zhang, J.; Zhang, A.; Peng, J. Evaluation on deformation behavior of granular base material during repeated load triaxial testing by discrete-element method. *Int. J. Geomech.* **2022**, *22*, 04022210. [CrossRef]
89. Sun, P.; Zhang, K.; Han, S.; Xiao, Y. Aggregate Geometrical Features and Their Influence on the Surface Properties of Asphalt Pavement. *Materials* **2022**, *15*, 3222. [CrossRef] [PubMed]
90. Wei, H.; Li, J.; Wang, F.; Zheng, J.; Tao, Y.; Zhang, Y. Numerical investigation on fracture evolution of asphalt mixture compared with acoustic emission. *Int. J. Pavement Eng.* **2022**, *23*, 3481–3491. [CrossRef]
91. Prudêncio, L.R., Jr.; Weidmann, D.F.; de Oliveira, A.L.; Damo, G.F. Particle shape analysis of fine aggregate using a simplified digital image processing method. *Mag. Concr. Res.* **2013**, *65*, 27–36. [CrossRef]
92. Airey, G.; Collop, A. Mechanical and structural assessment of laboratory-and field-compacted asphalt mixtures. *Int. J. Pavement Eng.* **2016**, *17*, 50–63. [CrossRef]
93. Cong, L.; Shi, J.; Wang, T.; Yang, F.; Zhu, T. A method to evaluate the segregation of compacted asphalt pavement by processing the images of paved asphalt mixture. *Constr. Build. Mater.* **2019**, *224*, 622–629. [CrossRef]
94. Li, P.; Ding, Z.; Rao, W. Evaluation of deformation properties of asphalt mixture using aggregate slip test. *Int. J. Pavement Eng.* **2016**, *17*, 542–549. [CrossRef]
95. Li, Q.J.; Zhan, Y.; Yang, G.; Wang, K.C. Pavement skid resistance as a function of pavement surface and aggregate texture properties. *Int. J. Pavement Eng.* **2020**, *21*, 1159–1169. [CrossRef]
96. Zhang, K.; Sun, P.; Li, L.; Zhao, Y.; Zhao, Y.; Zhang, Z. A novel evaluation method of aggregate distribution homogeneity for asphalt pavement based on the characteristics of texture structure. *Constr. Build. Mater.* **2021**, *306*, 124927. [CrossRef]
97. Xing, C.; Xu, H.; Tan, Y.; Liu, X.; Ye, Q. Mesostructured property of aggregate disruption in asphalt mixture based on digital image processing method. *Constr. Build. Mater.* **2019**, *200*, 781–789. [CrossRef]
98. Ding, L.; Zhang, J.; Zhou, C.; Han, S.; Du, Q. Particle breakage investigation of construction waste recycled aggregates in subgrade application scenario. *Powder Technol.* **2022**, *404*, 117448. [CrossRef]
99. You, T.; Al-Rub, R.K.A.; Masad, E.A.; Little, D.N. Three-dimensional microstructural modeling of asphalt concrete by use of X-ray computed tomography. *Transp. Res. Rec.* **2013**, *2373*, 63–70. [CrossRef]
100. Tashman, L.; Masad, E.; D'Angelo, J.; Bukowski, J.; Harman, T. X-ray tomography to characterize air void distribution in superpave gyratory compacted specimens. *Int. J. Pavement Eng.* **2002**, *3*, 19–28. [CrossRef]
101. Zhang, C.; Wang, H.; You, Z.; Yang, X. Compaction characteristics of asphalt mixture with different gradation type through Superpave Gyratory Compaction and X-ray CT Scanning. *Constr. Build. Mater.* **2016**, *129*, 243–255. [CrossRef]
102. Hu, J.; Qian, Z.; Liu, Y.; Zhang, M. High-temperature failure in asphalt mixtures using micro-structural investigation and image analysis. *Constr. Build. Mater.* **2015**, *84*, 136–145. [CrossRef]
103. Hu, J.; Qian, Z.; Liu, Y.; Xue, Y. Microstructural characteristics of asphalt concrete with different gradations by X-ray CT. *J. Wuhan Univ. Technol.-Mater. Sci. Ed.* **2017**, *32*, 625–632. [CrossRef]
104. Yang, X.; You, Z.; Wang, Z.; Dai, Q. Review on heterogeneous model reconstruction of stone-based composites in numerical simulation. *Constr. Build. Mater.* **2016**, *117*, 229–243. [CrossRef]
105. Liu, Y.; You, Z. Discrete-element modeling: Impacts of aggregate sphericity, orientation, and angularity on creep stiffness of idealized asphalt mixtures. *J. Eng. Mech.* **2011**, *137*, 294–303. [CrossRef]
106. Tan, L.; Xiao, J.; Singh, A. Finite Element Analysis on the Uniaxial Compressive Behavior of Concrete with Large-Size Recycled Coarse Aggregate. *J. Renew. Mater.* **2022**, *10*, 699.
107. Kurumatani, M.; Terada, K.; Kato, J.; Kyoya, T.; Kashiyama, K. An isotropic damage model based on fracture mechanics for concrete. *Eng. Fract. Mech.* **2016**, *155*, 49–66. [CrossRef]
108. Bencardino, F.; Condello, A.; Ombres, L. Numerical and analytical modeling of concrete beams with steel, FRP and hybrid FRP-steel reinforcements. *Compos. Struct.* **2016**, *140*, 53–65. [CrossRef]
109. Gong, F.; Liu, Y.; Zhou, X.; You, Z. Lab assessment and discrete element modeling of asphalt mixture during compaction with elongated and flat coarse aggregates. *Constr. Build. Mater.* **2018**, *182*, 573–579. [CrossRef]
110. Kutay, M.E.; Varma, S.; Jamrah, A. A micromechanical model to create digital microstructures of asphalt mastics and crumb rubber-modified binders. *Int. J. Pavement Eng.* **2017**, *18*, 754–764. [CrossRef]
111. Liu, Y.; You, Z. Simulation of cyclic loading tests for asphalt mixtures using user defined models within discrete element method. In *GeoCongress 2008: Characterization, Monitoring, and Modeling of Geosystems*; American Society of Civil Engineers: Reston, VA, USA, 2008; pp. 742–749.
112. Liu, Y.; You, Z. Visualization and simulation of asphalt concrete with randomly generated three-dimensional models. *J. Comput. Civ. Eng.* **2009**, *23*, 340–347. [CrossRef]
113. Wang, X.; Liang, Z.; Nie, Z.; Gong, J. Stochastic numerical model of stone-based materials with realistic stone-inclusion features. *Constr. Build. Mater.* **2019**, *197*, 830–848. [CrossRef]
114. Harthong, B.; Jérier, J.F.; Dorémus, P.; Imbault, D.; Donzé, F.V. Modeling of high-density compaction of granular materials by the discrete element method. *Int. J. Solids Struct.* **2009**, *46*, 3357–3364. [CrossRef]
115. Liu, Y.; Zhou, X.; You, Z.; Yao, S.; Gong, F.; Wang, H. Discrete element modeling of realistic particle shapes in stone-based mixtures through MATLAB-based imaging process. *Constr. Build. Mater.* **2017**, *143*, 169–178. [CrossRef]
116. Wang, L.; Park, J.Y.; Fu, Y. Representation of real particles for DEM simulation using X-ray tomography. *Constr. Build. Mater.* **2007**, *21*, 338–346. [CrossRef]

117. Latham, J.P.; Munjiza, A.; Garcia, X.; Xiang, J.; Guises, R. Three-dimensional particle shape acquisition and use of shape library for DEM and FEM/DEM simulation. *Miner. Eng.* **2008**, *21*, 797–805. [CrossRef]
118. Jensen, R.P.; Edil, T.B.; Bosscher, P.J.; Plesha, M.E.; Kahla, N.B. Effect of particle shape on interface behavior of DEM-simulated granular materials. *Int. J. Geomech.* **2001**, *1*, 1–19. [CrossRef]
119. Sobolev, K.; Amirjanov, A. The development of a simulation model of the dense packing of large particulate assemblies. *Powder Technol.* **2004**, *141*, 155–160. [CrossRef]
120. Gopalakrishnan, K.; Shashidhar, N. Structural characteristics of three-dimensional random packing of aggregates with wide size distribution. *Int. J. Civ. Environ. Eng.* **2007**, *1*, 78–85.
121. Fu, G.; Dekelbab, W. 3-D random packing of polydisperse particles and concrete aggregate grading. *Powder Technol.* **2003**, *133*, 147–155. [CrossRef]
122. Liu, L.; Shen, D.; Chen, H.; Xu, W. Aggregate shape effect on the diffusivity of mortar: A 3D numerical investigation by random packing models of ellipsoidal particles and of convex polyhedral particles. *Comput. Struct.* **2014**, *144*, 40–51. [CrossRef]
123. He, H.; Guo, Z.; Stroeven, P.; Stroeven, M.; Sluys, L.J. Characterization of the packing of aggregate in concrete by a discrete element approach. *Mater. Charact.* **2009**, *60*, 1082–1087. [CrossRef]
124. Du, C.B.; Sun, L.G. Numerical simulation of aggregate shapes of two-dimensional concrete and its application. *J. Aerosp. Eng.* **2007**, *20*, 172–178. [CrossRef]
125. Ma, H.; Xu, W.; Li, Y. Random aggregate model for mesoscopic structures and mechanical analysis of fully-graded concrete. *Comput. Struct.* **2016**, *177*, 103–113. [CrossRef]
126. Liu, B.; Bai, G.L.; Xu, Z.H.; Ma, J.F.; Han, Y.Y. Experimental study and finite element modeling of bond behavior between recycled aggregate concrete and the shaped steel. *Eng. Struct.* **2019**, *201*, 109840. [CrossRef]
127. Ferellec, J.F.; McDowell, G. A simple method to create complex particle shapes for DEM. *Geomech. Geoengin. Int. J.* **2008**, *3*, 211–216. [CrossRef]
128. Yang, X.; You, Z.; Jin, C.; Wang, H. Aggregate representation for mesostructure of stone based materials using a sphere growth model based on realistic aggregate shapes. *Mater. Struct.* **2016**, *49*, 2493–2508. [CrossRef]
129. Zhou, R.; Song, Z.; Lu, Y. 3D mesoscale finite element modelling of concrete. *Comput. Struct.* **2017**, *192*, 96–113. [CrossRef]
130. Yu, Y.; Zheng, Y.; Guo, Y.; Hu, S.; Hua, K. Mesoscale finite element modeling of recycled aggregate concrete under axial tension. *Constr. Build. Mater.* **2021**, *266*, 121002. [CrossRef]
131. Coleri, E.; Harvey, J.T.; Yang, K.; Boone, J.M. Development of a micromechanical finite element model from computed tomography images for shear modulus simulation of asphalt mixtures. *Constr. Build. Mater.* **2012**, *30*, 783–793. [CrossRef]
132. Souza, L.T.; Kim, Y.R.; Souza, F.V.; Castro, L.S. Experimental testing and finite-element modeling to evaluate the effects of aggregate angularity on bituminous mixture performance. *J. Mater. Civ. Eng.* **2012**, *24*, 249–258. [CrossRef]
133. Shahbeyk, S.; Hosseini, M.; Yaghoobi, M. Mesoscale finite element prediction of concrete failure. *Comput. Mater. Sci.* **2011**, *50*, 1973–1990. [CrossRef]
134. Wang, Z.; Kwan, A.; Chan, H. Mesoscopic study of concrete I: Generation of random aggregate structure and finite element mesh. *Comput. Struct.* **1999**, *70*, 533–544. [CrossRef]
135. Peng, Z.; Doroodchi, E.; Moghtaderi, B. Heat transfer modelling in Discrete Element Method (DEM)-based simulations of thermal processes: Theory and model development. *Prog. Energy Combust. Sci.* **2020**, *79*, 100847. [CrossRef]
136. Zhang, T.; Zhang, C.; Zou, J.; Wang, B.; Song, F.; Yang, W. DEM exploration of the effect of particle shape on particle breakage in granular assemblies. *Comput. Geotech.* **2020**, *122*, 103542. [CrossRef]
137. Wang, X.; Yin, Z.Y.; Su, D.; Wu, X.; Zhao, J. A novel approach of random packing generation of complex-shaped 3D particles with controllable sizes and shapes. *Acta Geotech.* **2022**, *17*, 355–376. [CrossRef]
138. Wang, X.; Nie, Z.; Gong, J.; Liang, Z. Random generation of convex aggregates for DEM study of particle shape effect. *Constr. Build. Mater.* **2021**, *268*, 121468. [CrossRef]
139. Collop, A.C.; McDowell, G.R.; Lee, Y. Use of the distinct element method to model the deformation behavior of an idealized asphalt mixture. *Int. J. Pavement Eng.* **2004**, *5*, 1–7. [CrossRef]
140. Collop, A.C.; McDowell, G.R.; Lee, Y.W. Modelling dilation in an idealised asphalt mixture using discrete element modelling. *Granul. Matter* **2006**, *8*, 175–184. [CrossRef]
141. You, Z.; Adhikari, S.; Dai, Q. Three-dimensional discrete element models for asphalt mixtures. *J. Eng. Mech.* **2008**, *134*, 1053–1063. [CrossRef]
142. Wang, X.; Yin, Z.Y.; Xiong, H.; Su, D.; Feng, Y.T. A spherical-harmonic-based approach to discrete element modeling of 3D irregular particles. *Int. J. Numer. Methods Eng.* **2021**, *122*, 5626–5655. [CrossRef]
143. Dondi, G.; Simone, A.; Vignali, V.; Manganelli, G. Numerical and experimental study of granular mixes for asphalts. *Powder Technol.* **2012**, *232*, 31–40. [CrossRef]
144. Ferellec, J.F.; McDowell, G.R. A method to model realistic particle shape and inertia in DEM. *Granul. Matter* **2010**, *12*, 459–467. [CrossRef]
145. Fu, Y.; Wang, L.; Zhou, C. 3D clustering DEM simulation and non-invasive experimental verification of shear localisation in irregular particle assemblies. *Int. J. Pavement Eng.* **2010**, *11*, 355–365. [CrossRef]
146. He, H.; Stroeven, P.; Pirard, E.; Courard, L. On the shape simulation of aggregate and cement particles in a DEM system. *Adv. Mater. Sci. Eng.* **2015**, *2015*, 692768. [CrossRef]

147. Zhang, D.; Huang, X.; Zhao, Y. Algorithms for generating three-dimensional aggregates and asphalt mixture samples by the discrete-element method. *J. Comput. Civ. Eng.* **2013**, *27*, 111–117. [CrossRef]
148. Yao, Y.; Li, J.; Liang, C.; Hu, X. Effect of coarse recycled aggregate on failure strength for asphalt mixture using experimental and DEM method. *Coatings* **2021**, *11*, 1234. [CrossRef]
149. Yao, Y.; Li, J.; Ni, J.; Liang, C.; Zhang, A. Effects of gravel content and shape on shear behaviour of soil-rock mixture: Experiment and DEM modelling. *Comput. Geotech.* **2022**, *141*, 104476. [CrossRef]
150. Sherzer, G.L.; Alghalandis, Y.F.; Peterson, K. Introducing fracturing through aggregates in LDPM. *Eng. Fract. Mech.* **2022**, *261*, 108228. [CrossRef]
151. Sherzer, G.L.; Alghalandis, Y.F.; Peterson, K.; Shah, S. Comparative study of scale effect in concrete fracturing via Lattice Discrete Particle and Finite Discrete Element Models. *Eng. Fail. Anal.* **2022**, *135*, 106062. [CrossRef]
152. Naderi, S.; Tu, W.; Zhang, M. Meso-scale modelling of compressive fracture in concrete with irregularly shaped aggregates. *Cem. Concr. Res.* **2021**, *140*, 106317. [CrossRef]
153. Xing, C.; Xu, H.; Tan, Y.; Liu, X.; Zhou, C.; Scarpas, T. Gradation measurement of asphalt mixture by X-ray CT images and digital image processing methods. *Measurement* **2019**, *132*, 377–386. [CrossRef]
154. Chen, J.; Huang, B.; Shu, X. Air-void distribution analysis of asphalt mixture using discrete element method. *J. Mater. Civ. Eng.* **2013**, *25*, 1375–1385. [CrossRef]
155. Dubois, V.; De La Roche, C.; Burban, O. Influence of the compaction process on the air void homogeneity of asphalt mixtures samples. *Constr. Build. Mater.* **2010**, *24*, 885–897. [CrossRef]
156. Liu, P.; Hu, J.; Falla, G.C.; Wang, D.; Leischner, S.; Oeser, M. Primary investigation on the relationship between microstructural characteristics and the mechanical performance of asphalt mixtures with different compaction degrees. *Constr. Build. Mater.* **2019**, *223*, 784–793. [CrossRef]
157. Park, S.B.; Seo, D.S.; Lee, J. Studies on the sound absorption characteristics of porous concrete based on the content of recycled aggregate and target void ratio. *Cem. Concr. Res.* **2005**, *35*, 1846–1854. [CrossRef]
158. Aliha, M.; Fattahi Amirdehi, H. Fracture toughness prediction using Weibull statistical method for asphalt mixtures containing different air void contents. *Fatigue Fract. Eng. Mater. Struct.* **2017**, *40*, 55–68. [CrossRef]
159. Golalipour, A.; Jamshidi, E.; Niazi, Y.; Afsharikia, Z.; Khadem, M. Effect of aggregate gradation on rutting of asphalt pavements. *Procedia-Soc. Behav. Sci.* **2012**, *53*, 440–449. [CrossRef]
160. Elliott, R.P.; Ford, M.C., Jr.; Ghanim, M.; Tu, Y.F. Effect of aggregate gradation variation on asphalt concrete mix properties. *Transp. Res. Rec.* **1991**, *1317*, 52–60.
161. Hunter, A.E.; McGreavy, L.; Airey, G.D. Effect of compaction mode on the mechanical performance and variability of asphalt mixtures. *J. Transp. Eng.* **2009**, *135*, 839–851. [CrossRef]
162. Pérez-Jiménez, F.; Martínez, A.H.; Miró, R.; Hernández-Barrera, D.; Araya-Zamorano, L. Effect of compaction temperature and procedure on the design of asphalt mixtures using Marshall and gyratory compactors. *Constr. Build. Mater.* **2014**, *65*, 264–269. [CrossRef]
163. Dan, H.C.; Yang, D.; Zhao, L.H.; Wang, S.P.; Zhang, Z. Meso-scale study on compaction characteristics of asphalt mixtures in Superpave gyratory compaction using SmartRock sensors. *Constr. Build. Mater.* **2020**, *262*, 120874. [CrossRef]
164. Wei, H.; Bai, X.P.; Wang, F.Y.; Li, W.; Jin, J. Mixing ratio design of emulsified asphalt cold recycled mixture based on gyratory compaction molding. *J. Cent. South Univ.* **2019**, *26*, 759–767.
165. Şengün, E.; Alam, B.; Shabani, R.; Yaman, I. The effects of compaction methods and mix parameters on the properties of roller compacted concrete mixtures. *Constr. Build. Mater.* **2019**, *228*, 116807. [CrossRef]
166. Awed, A.; Kassem, E.; Masad, E.; Little, D. Method for predicting the laboratory compaction behavior of asphalt mixtures. *J. Mater. Civ. Eng.* **2015**, *27*, 04015016. [CrossRef]
167. Coenen, A.R.; Kutay, M.E.; Sefidmazgi, N.R.; Bahia, H.U. Aggregate structure characterisation of asphalt mixtures using two-dimensional image analysis. *Road Mater. Pavement Des.* **2012**, *13*, 433–454. [CrossRef]
168. Chang, J.; Li, J.; Hu, H.; Qian, J.; Yu, M. Numerical investigation on aggregate segregation of Superpave gyratory compaction and its influence on mechanical properties of asphalt mixtures. *J. Mater. Civ. Eng.* **2022**, *in press*.
169. Hassan, N.A.; Airey, G.D.; Khan, R.; Collop, A.C. Nondestructive characterisation of the effect of asphalt mixture compaction on aggregate orientation and segregation using X-ray computed tomography. *Int. J. Pavement Res. Technol.* **2012**, *5*, 84.
170. Jiang, S.; Shen, L. Aggregate shape effect on fracture and breakage of cementitious granular materials. *Int. J. Mech. Sci.* **2022**, *220*, 107161. [CrossRef]
171. Zhang, J.; Gu, F.; Zhang, Y. Use of building-related construction and demolition wastes in highway embankment: Laboratory and field evaluations. *J. Clean. Prod.* **2019**, *230*, 1051–1060. [CrossRef]
172. Bektas, F.; Wang, K.; Ceylan, H. Effects of crushed clay brick aggregate on mortar durability. *Constr. Build. Mater.* **2009**, *23*, 1909–1914. [CrossRef]
173. Mostofinejad, D.; Reisi, M. A new DEM-based method to predict packing density of coarse aggregates considering their grading and shapes. *Constr. Build. Mater.* **2012**, *35*, 414–420. [CrossRef]
174. Li, J.; Huang, Y.; Pu, H.; Gao, H.; Li, Y.; Ouyang, S.; Guo, Y. Influence of block shape on macroscopic deformation response and meso-fabric evolution of crushed gangue under the triaxial compression. *Powder Technol.* **2021**, *384*, 112–124. [CrossRef]

175. Zhao, L.; Zhang, S.; Huang, D.; Wang, X.; Zhang, Y. 3D shape quantification and random packing simulation of rock aggregates using photogrammetry-based reconstruction and discrete element method. *Constr. Build. Mater.* **2020**, *262*, 119986. [CrossRef]
176. Wu, J.; Zhou, X.; Zeng, X.; Xie, Y.; Long, G.; Dong, R.; Umar, H.A.; Ma, G.; Yao, L. Effect of aggregate morphology characteristics on the voidage of aggregate loose packing based on 3D discrete element method. *Constr. Build. Mater.* **2022**, *348*, 128598. [CrossRef]
177. Rocco, C.; Elices, M. Effect of aggregate shape on the mechanical properties of a simple concrete. *Eng. Fract. Mech.* **2009**, *76*, 286–298. [CrossRef]
178. Jaya, R.P.; Hassan, N.A.; Mahmud, M.Z.H.; Aziz, M.M.A.; Hamzah, M.O.; Wan, C.N.C. Effect of aggregate shape on the properties of asphaltic concrete AC14. *J. Teknol.* **2014**, *71*, 69–73.
179. Sun, Y.; Zhang, Z.; Wei, X.; Du, C.; Gong, M.; Chen, J.; Gong, H. Mesomechanical prediction of viscoelastic behavior of asphalt concrete considering effect of aggregate shape. *Constr. Build. Mater.* **2021**, *274*, 122096. [CrossRef]
180. Sengoz, B.; Onsori, A.; Topal, A. Effect of aggregate shape on the surface properties of flexible pavement. *KSCE J. Civ. Eng.* **2014**, *18*, 1364–1371. [CrossRef]
181. Pouranian, M.R.; Shishehbor, M.; Haddock, J.E. Impact of the coarse aggregate shape parameters on compaction characteristics of asphalt mixtures. *Powder Technol.* **2020**, *363*, 369–386. [CrossRef]
182. Cook, C.S.; Tanyu, B.F.; Yavuz, A.B. Effect of particle shape on durability and performance of unbound aggregate base. *J. Mater. Civ. Eng.* **2017**, *29*, 04016221. [CrossRef]
183. Singh, D.; Zaman, M.; Commuri, S. Effect of production and sample preparation methods on aggregate shape parameters. *Int. J. Pavement Eng.* **2013**, *14*, 154–175. [CrossRef]
184. Ghabchi, R.; Zaman, M.; Kazmee, H.; Singh, D. Effect of shape parameters and gradation on laboratory-measured permeability of aggregate bases. *Int. J. Geomech.* **2015**, *15*, 04014070. [CrossRef]
185. Piotrowska, E.; Malecot, Y.; Ke, Y. Experimental investigation of the effect of coarse aggregate shape and composition on concrete triaxial behavior. *Mech. Mater.* **2014**, *79*, 45–57. [CrossRef]
186. Grigorovitch, M.; Gal, E.; Waisman, H. Embedded unit cell homogenization model for localized non-periodic elasto-plastic zones. *Comput. Mech.* **2021**, *68*, 1437–1456. [CrossRef]
187. Meng, Q.; Wang, H.; Xu, W.; Cai, M. A numerical homogenization study of the elastic property of a soil-rock mixture using random mesostructure generation. *Comput. Geotech.* **2018**, *98*, 48–57. [CrossRef]
188. Meng, Q.-X.; Lv, D.; Liu, Y. Mesoscale computational modeling of concrete-like particle-reinforced composites with non-convex aggregates. *Comput. Struct.* **2020**, *240*, 106349. [CrossRef]
189. Qian, G.; Hu, K.; Li, J.; Bai, X.; Li, N. Compaction process tracking for asphalt mixture using discrete element method. *Constr. Build. Mater.* **2020**, *235*, 117478. [CrossRef]
190. Alam, S.; Loukili, A.; Grondin, F. Monitoring size effect on crack opening in concrete by digital image correlation. *Eur. J. Environ. Civ. Eng.* **2012**, *16*, 818–836. [CrossRef]
191. Jin, L.; Yu, W.; Du, X.; Yang, W. Meso-scale simulations of size effect on concrete dynamic splitting tensile strength: Influence of aggregate content and maximum aggregate size. *Eng. Fract. Mech.* **2020**, *230*, 106979. [CrossRef]
192. Wang, X.-H.; Zhang, S.-R.; Wang, C.; Song, R.; Shang, C.; Fang, X. Experimental investigation of the size effect of layered roller compacted concrete (RCC) under high-strain-rate loading. *Constr. Build. Mater.* **2018**, *165*, 45–57. [CrossRef]